Introduction to the diamond NV centers focusing on quantum sensing applications

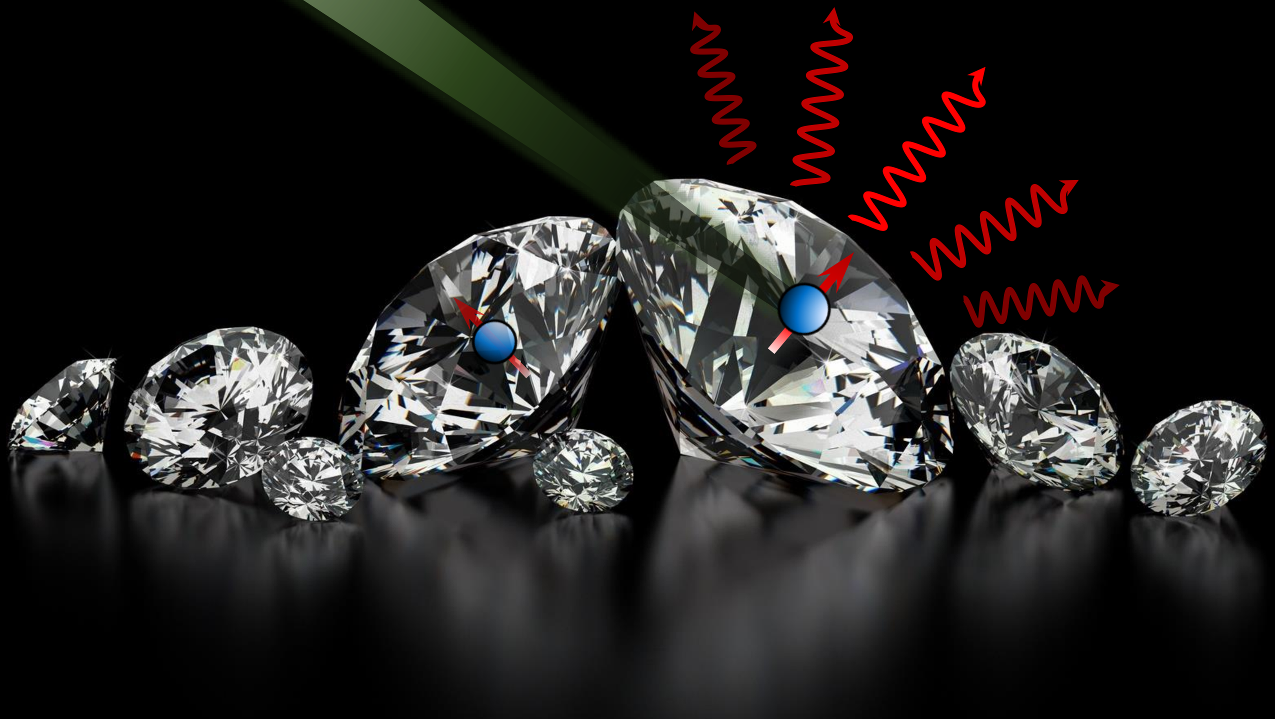

Donghun Lee

Department of Physics, Korea University

Toward quantum devices in real life

Quantum devices (applications of quantum systems)

e.g. quantum computers, quantum communications, quantum metrology

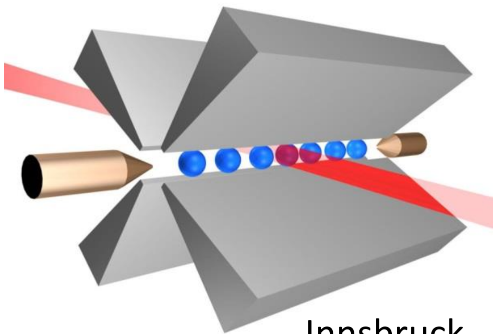

Innsbruck

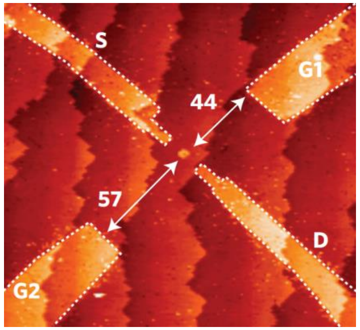

CQC

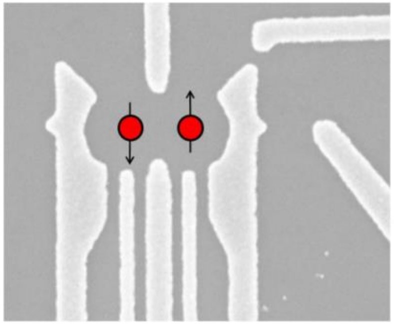

Harvard

Yale

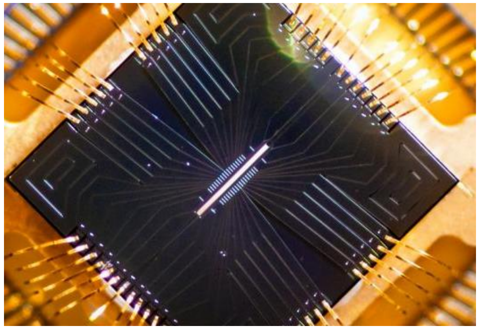

UMD

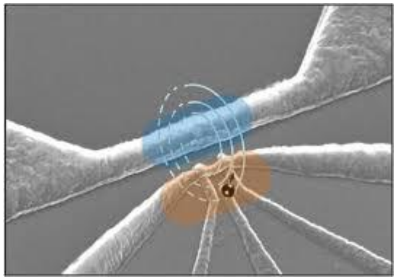

CQC

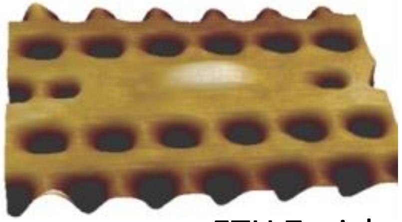

ETH Zurich

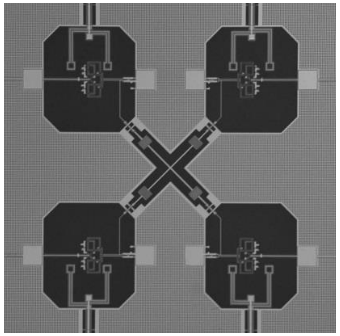

UCSB

- Long spin coherence time (e.g. trapped atoms)
- Fast processing capabilities (e.g. superconducting qubits)
- Scalabilities (e.g. solid-state QDs or defects)
- Interfaces and transducers (e.g. photons, mechanical oscillators)
- …

Toward quantum devices in real life

Quantum devices (applications of quantum systems)

e.g. quantum computers, quantum communications, quantum metrology

Nitrogen-Vacancy color centers in diamond crystal

“diamond NV centers”

- Lo
- Fa
- Sc
- Int ors)
- …

Outline

- Basics of the NV center
  - Structure, electronic, optical properties
  - Spin physics, coherence properties
- Applications for quantum metrology
  - Magnetic field sensing
  - Strain field sensing

Outline

- Basics of the NV center
    - Structure, electronic, optical properties
    - Spin physics, coherence properties
- Applications for quantum metrology
    - Magnetic field sensing
    - Strain field sensing

Physical structure of diamond and the NV center

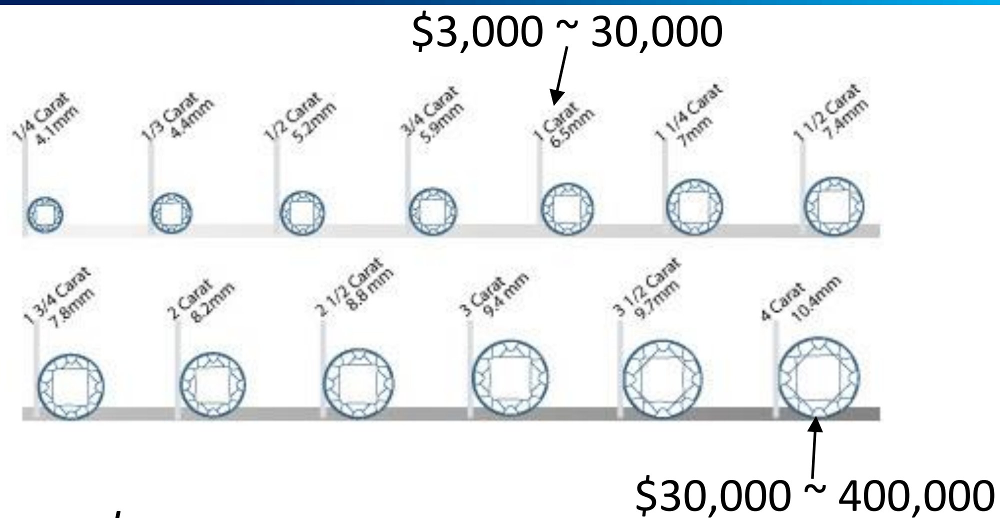

<u>Synthesized single crystal diamond for research</u>

- HPHT(high pressure high temperature) growth (> 50,000 bar, > 1400 ^{o}C)
- CVD(chemical vapor deposition) growth
- Nanodiamonds, thin films, bulk crystals…

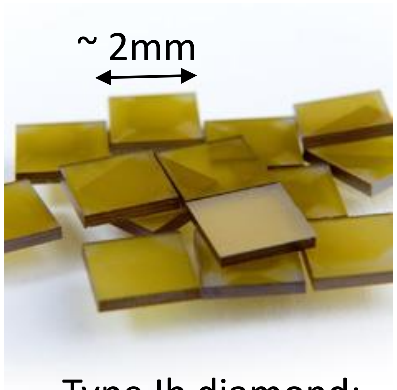

Type Ib diamond:
~ 100 ppm [N]

Element 6

Type IIa diamond: ~ 1 ppm [N]
Electronic grade: < 5 ppb [N]

Nanodiamonds

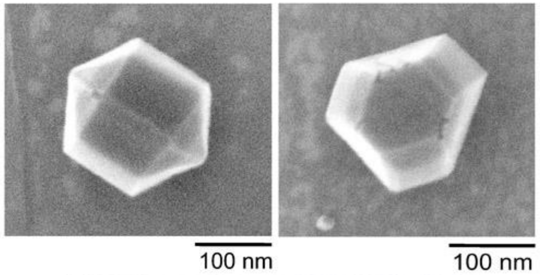

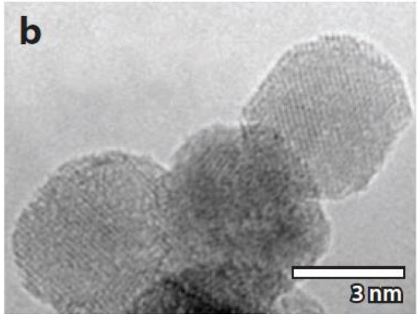

Physical structure of diamond and the NV center

Color centers in diamonds

- Pure diamond (clear)
- Nitrogen defects (yellow)
- Boron defects (blue)

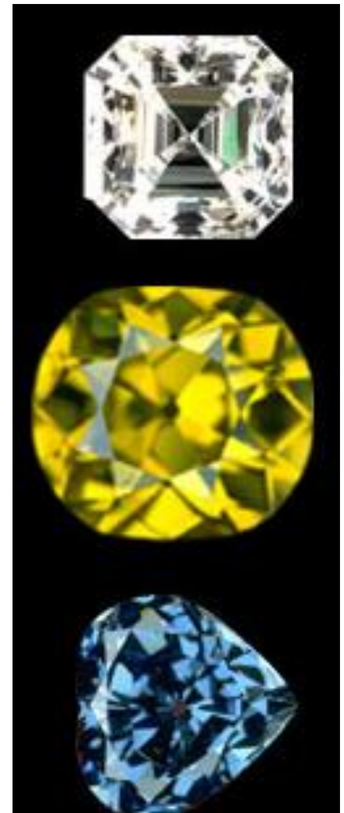

original-diamonds.com

- Nitrogen-Vacancy(NV) defects (pink)

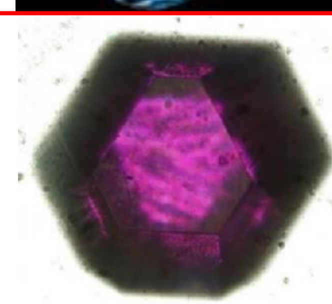

V. M. Acosta Ph.D. thesis (2011)

Formation of the NV center

- Natural or as-grown NV centers : longest spin coherence times for bulk NVs
- High density NV formation: electron irradiation (~ MeV) and annealing (~ 800 K)
- Low density NV formation: N implantation (~ keV) and annealing (~ 800 K)
- Position control of NV centers :
  - Depth control: delta-doped CVD growth
  - Lateral position control: masked implantation, TEM irradiation

<u>Delta-doped CVD growth</u>

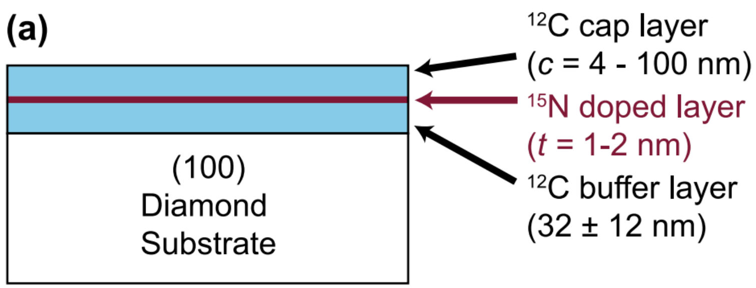

K. Ohno *et al.*, Appl. Phys. Lett. (2012)

<u>Masked implantation</u>

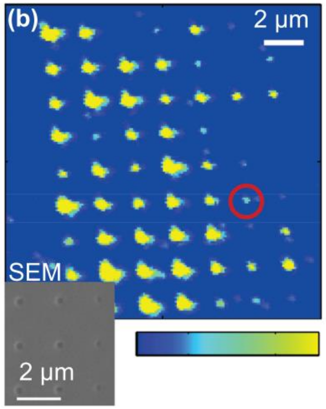

K. Ohno *et al.*, Appl. Phys. Lett. (2014)

<u>TEM irradiation</u>

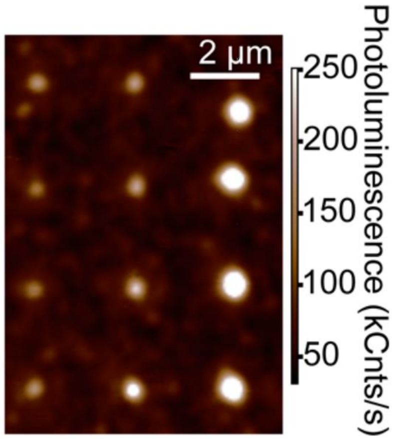

C. A. McLellan *et al.*, Nano Lett. (2016)

Fabrication of diamond nanostructures

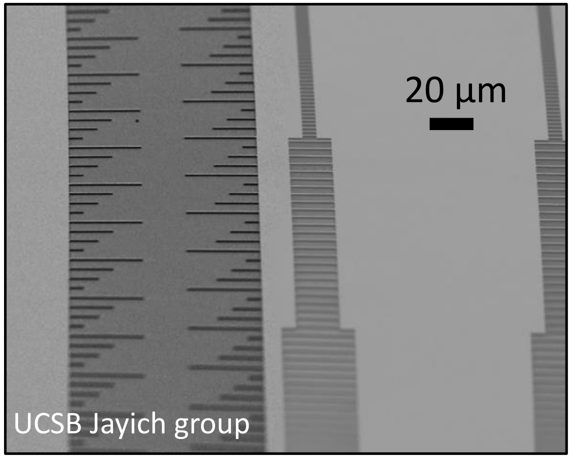

UCSB Jayich group

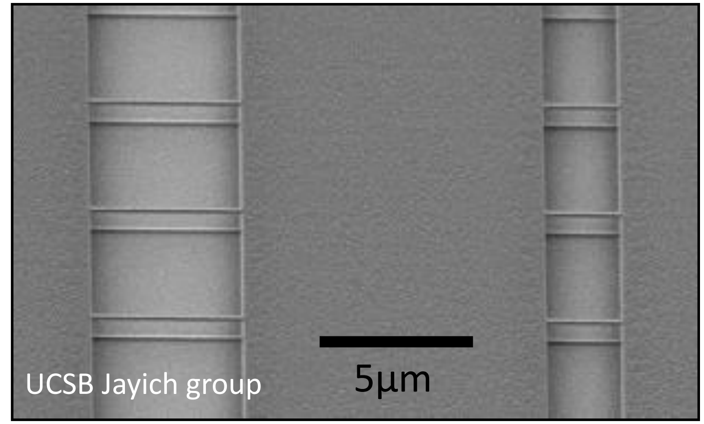

UCSB Jayich group

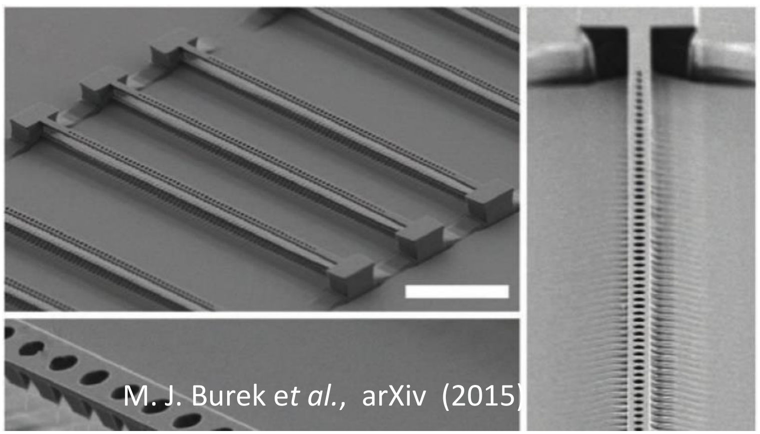
M. J. Burek et *al.*, arXiv (2015)

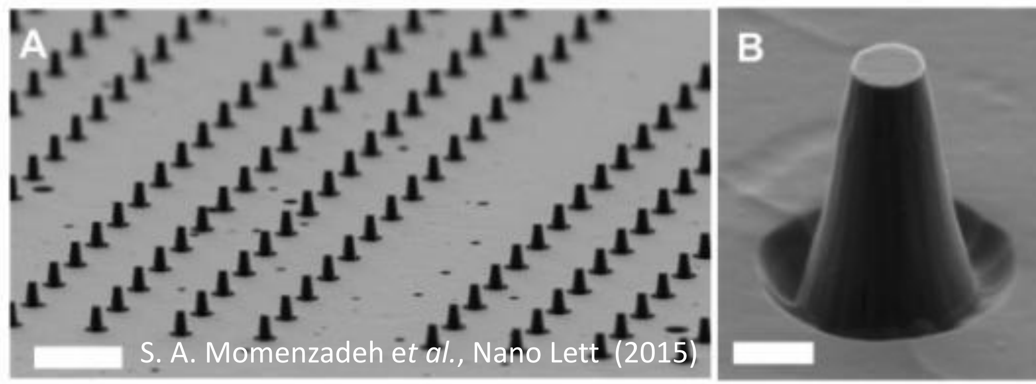

S. A. Momenzadeh et *al.*, Nano Lett (2015)

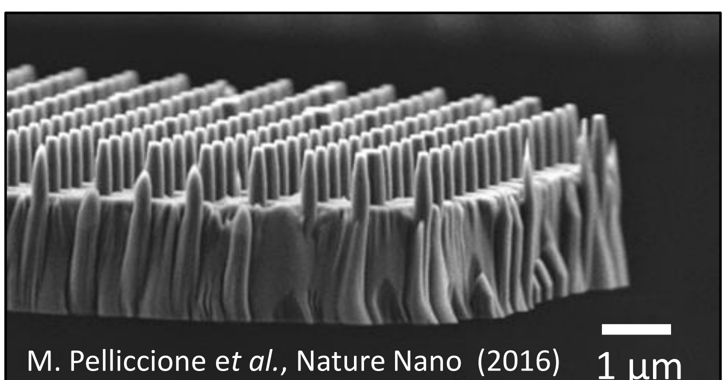

M. Pelliccione et *al.*, Nature Nano (2016)

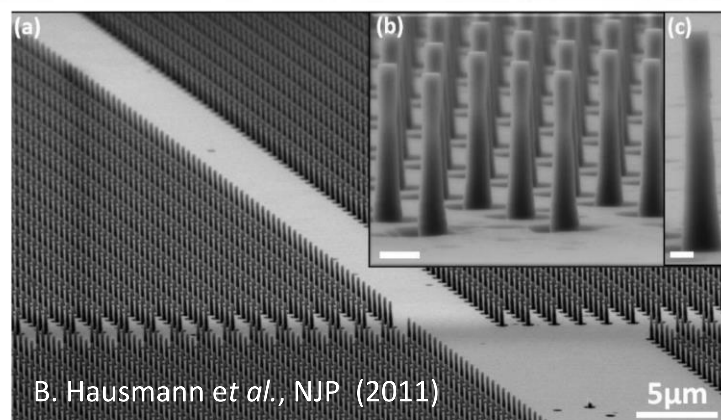

B. Hausmann et *al.*, NJP (2011)

Optical properties of the NV center

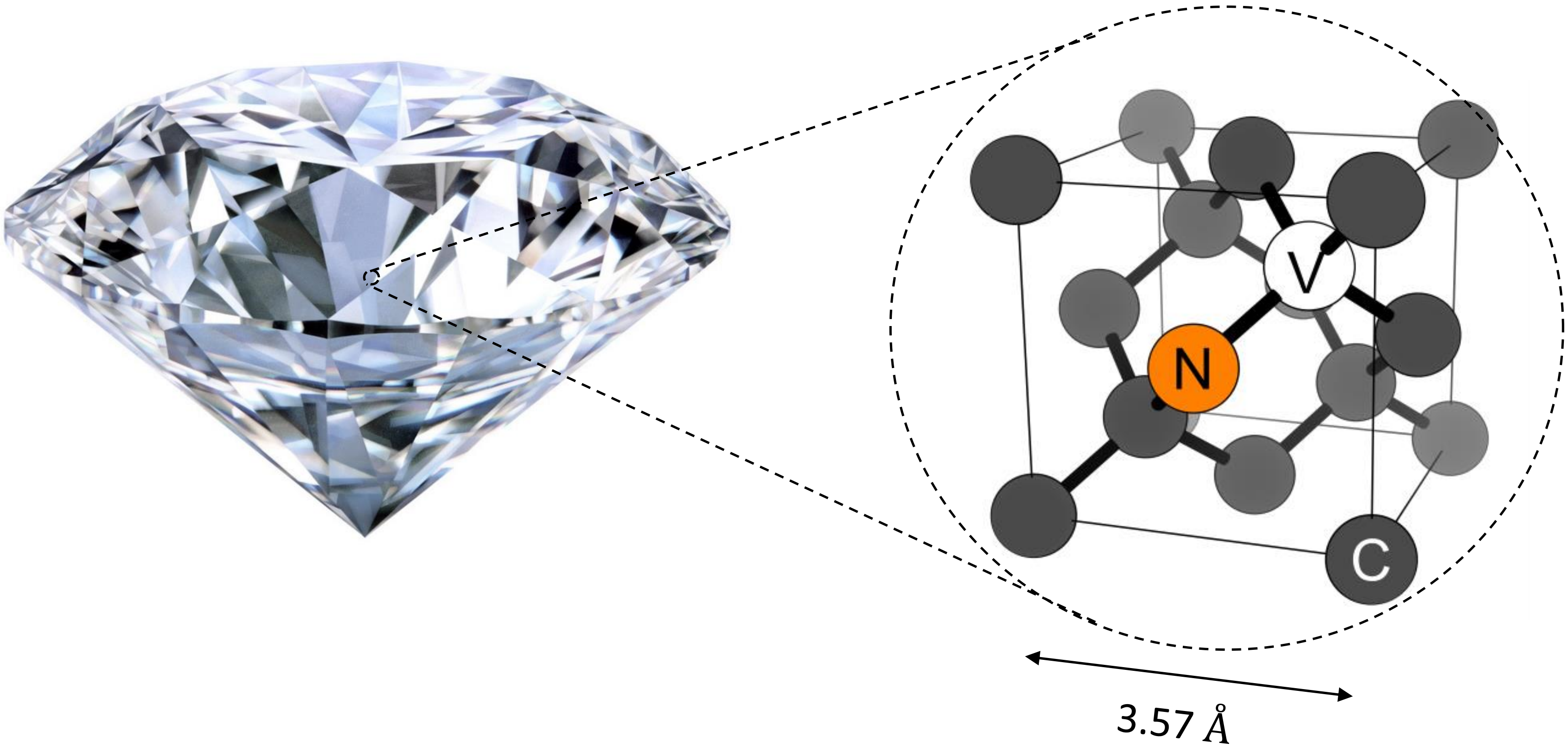

Optical properties of the NV center

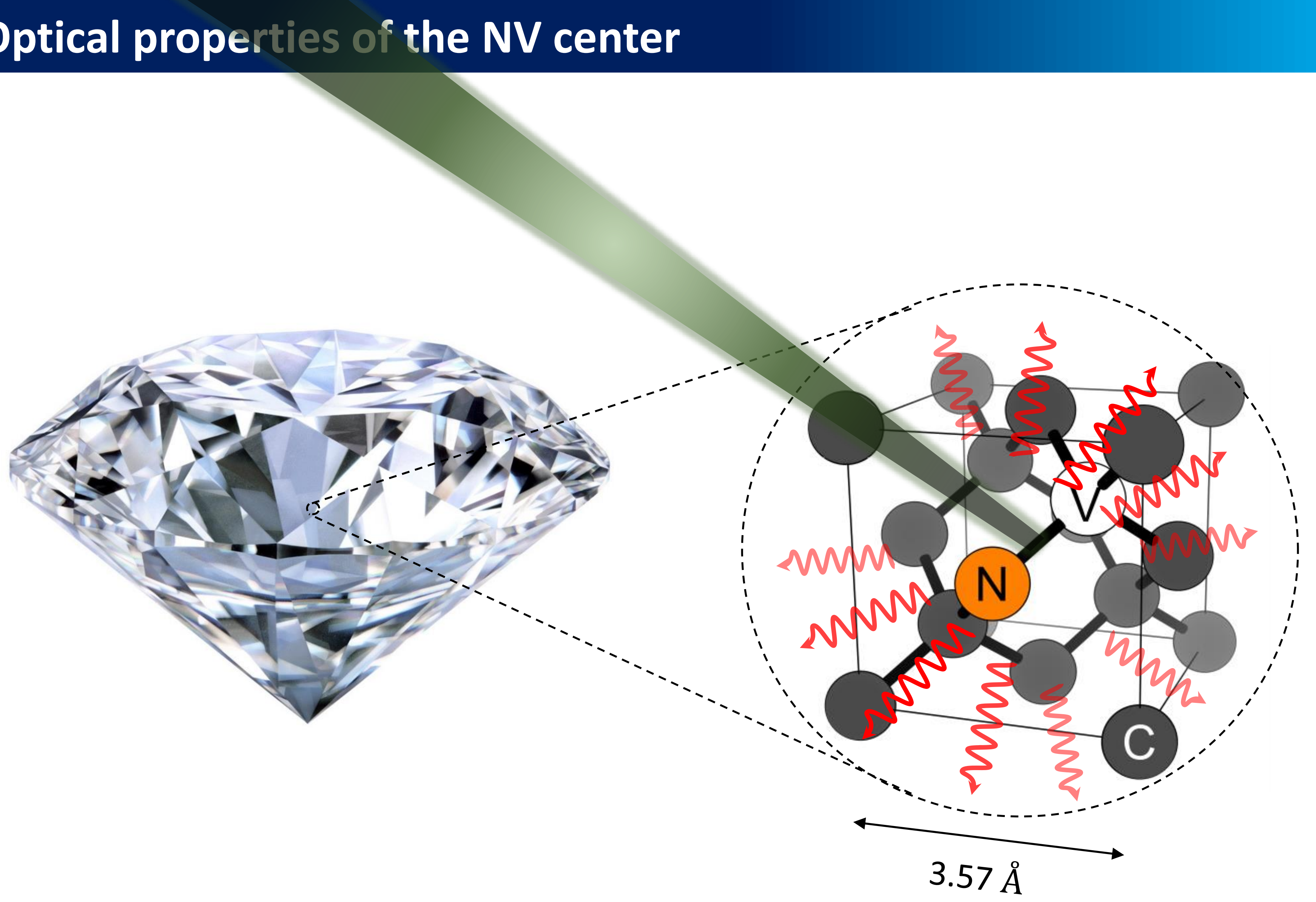

Optical properties of the NV center

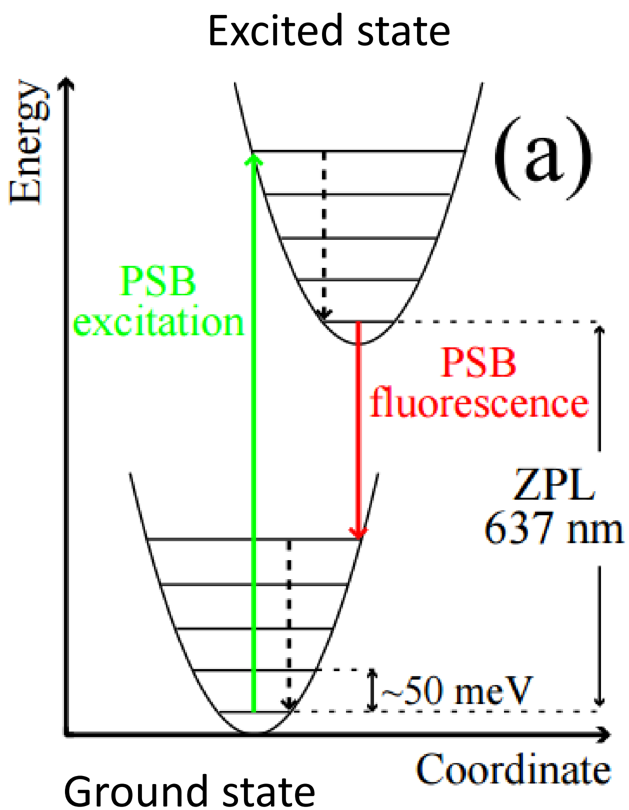

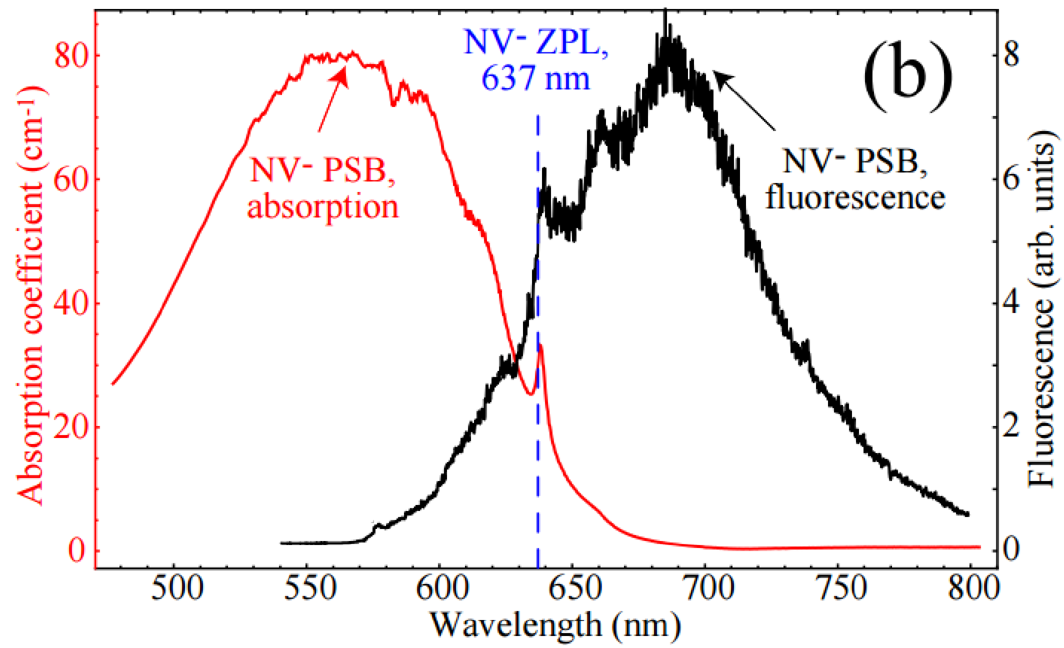

dashed lines : non-radiative decay

Room-temperature optical absorption and fluorescence (excited at 532 nm) spectra from NV^- center

V. M. Acosta Ph.D. thesis (2011)

Experimental setup: confocal optics

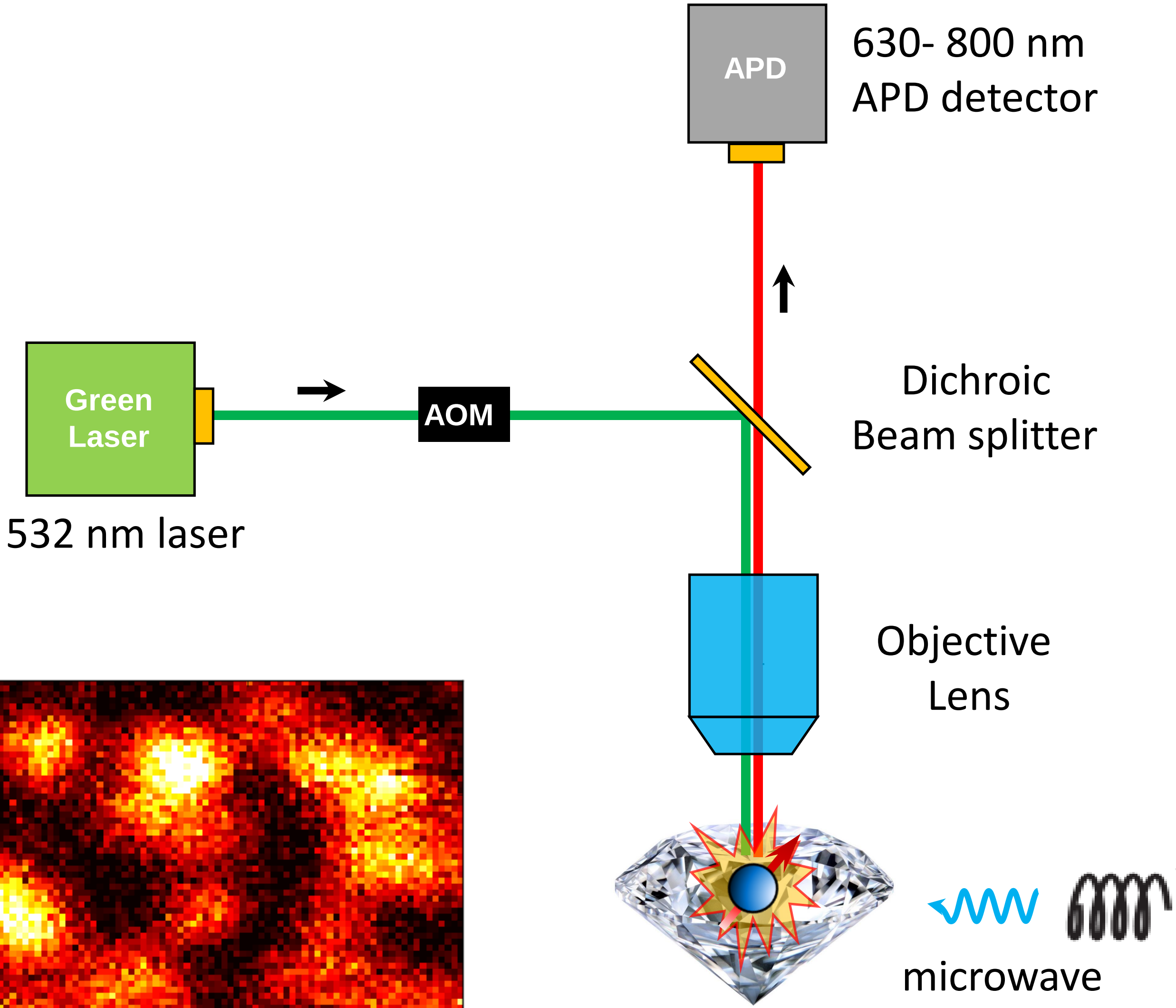

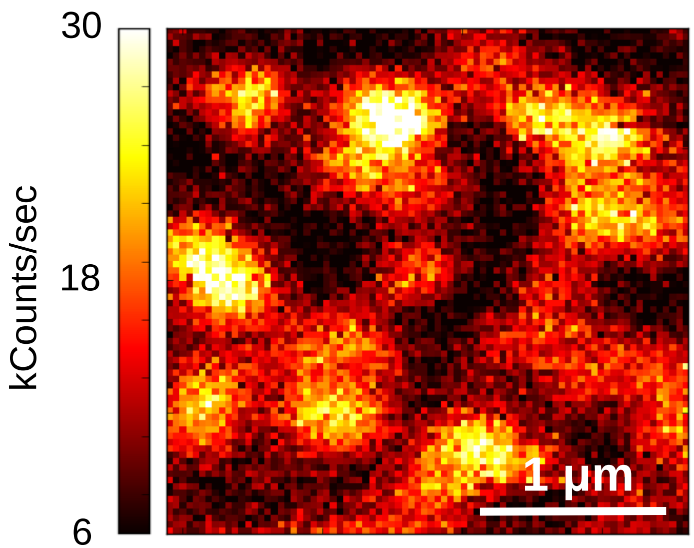

Electronic properties of the NV center

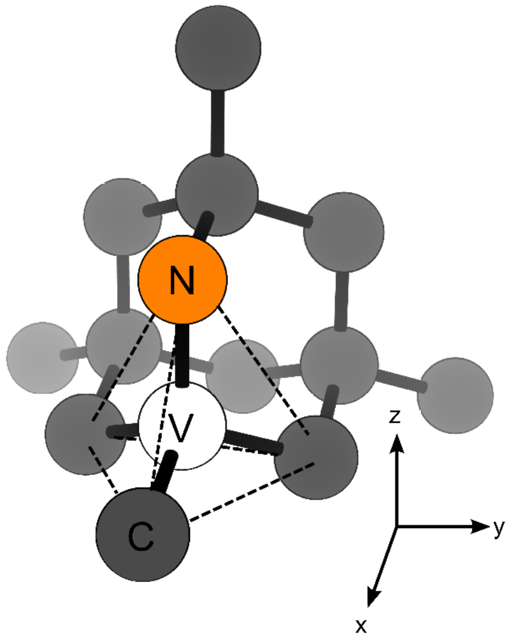

- LCAO (linear combinations of atomic orbitals) : four sp^3 dangling bonds
- C_{3v} point group symmetry

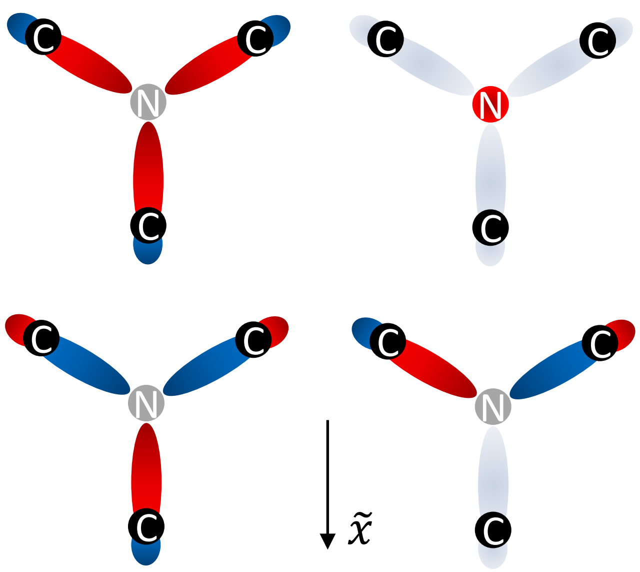

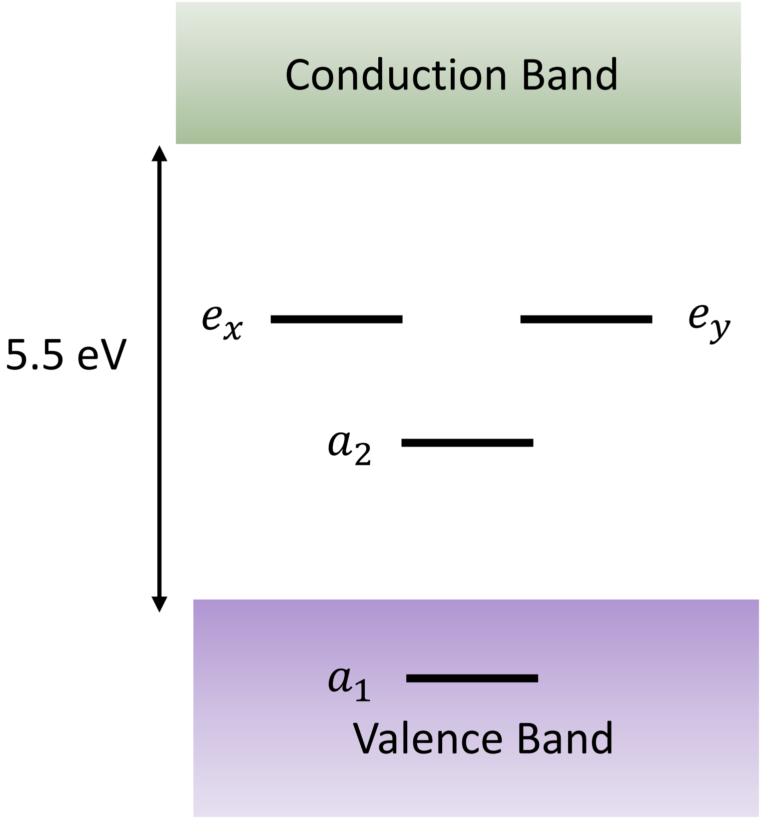

Electronic properties of the NV center

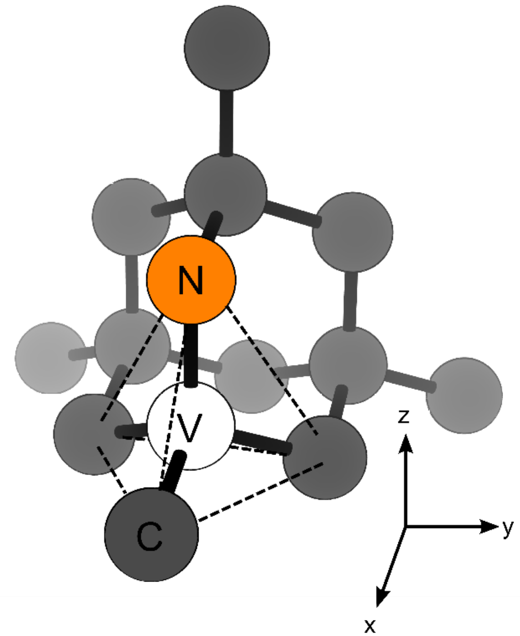

- LCAO (linear combinations of atomic orbitals)
  : four sp^3 dangling bonds
- C_{3v} point group symmetry
- There are total 6 electron for NV^-
  : 3 e^- from C, 2 e^- from N, 1 e^- from environment
- S = 1 (spin triplet) state

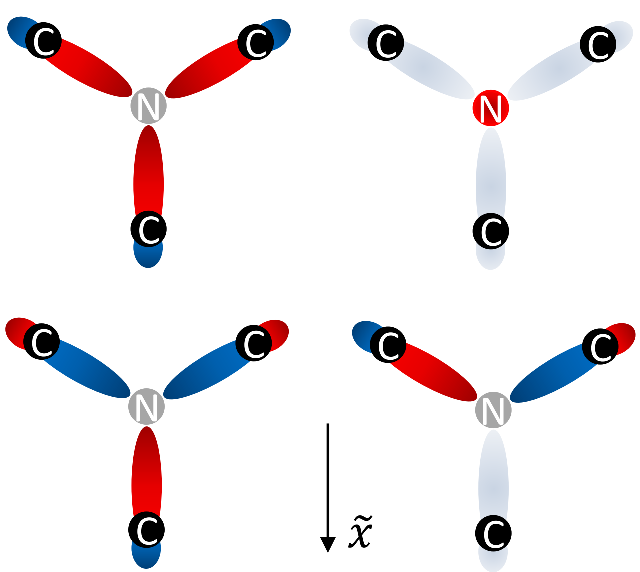

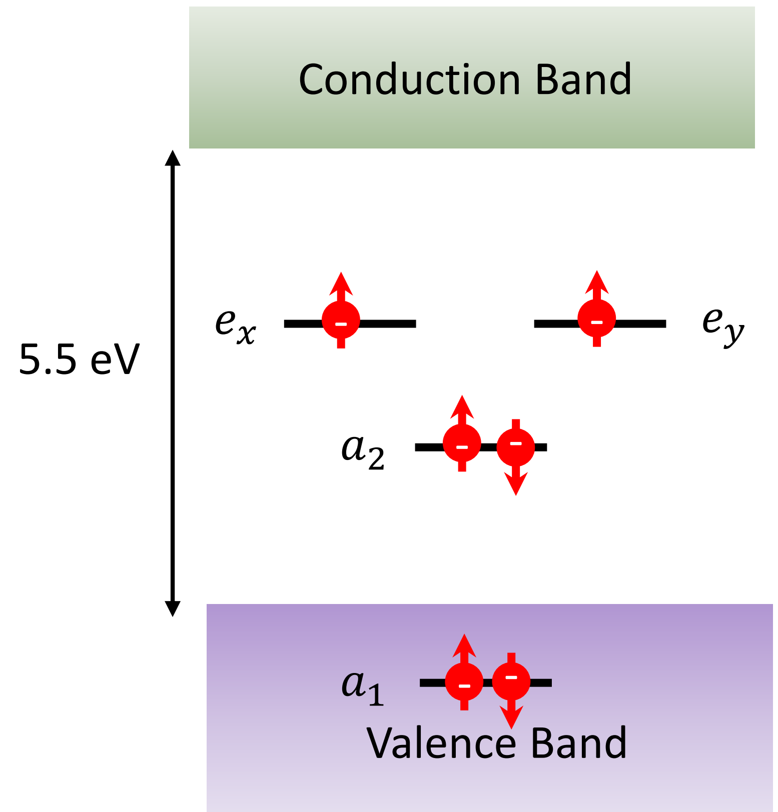

Electronic properties of the NV center

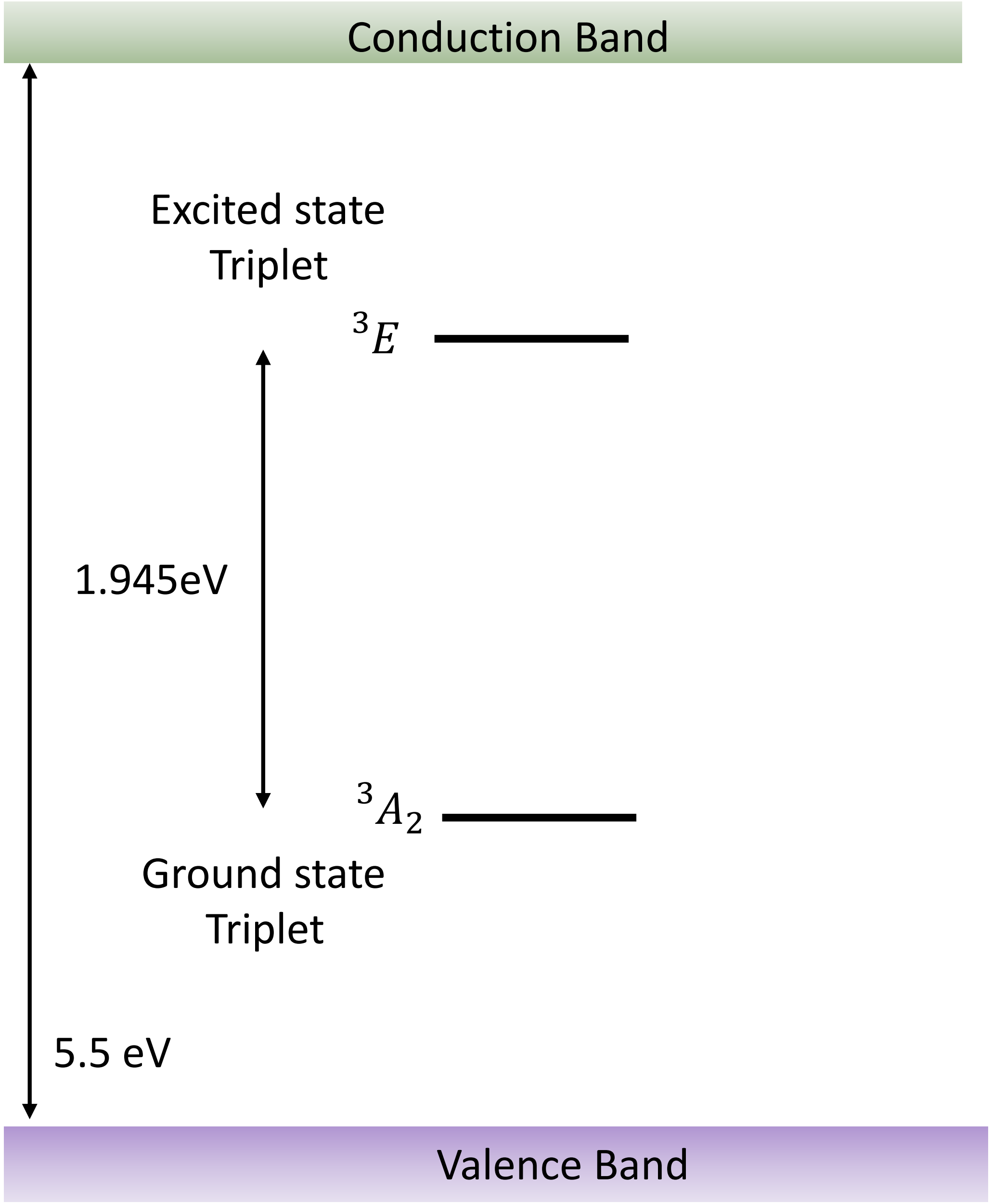

Electronic properties of the NV center

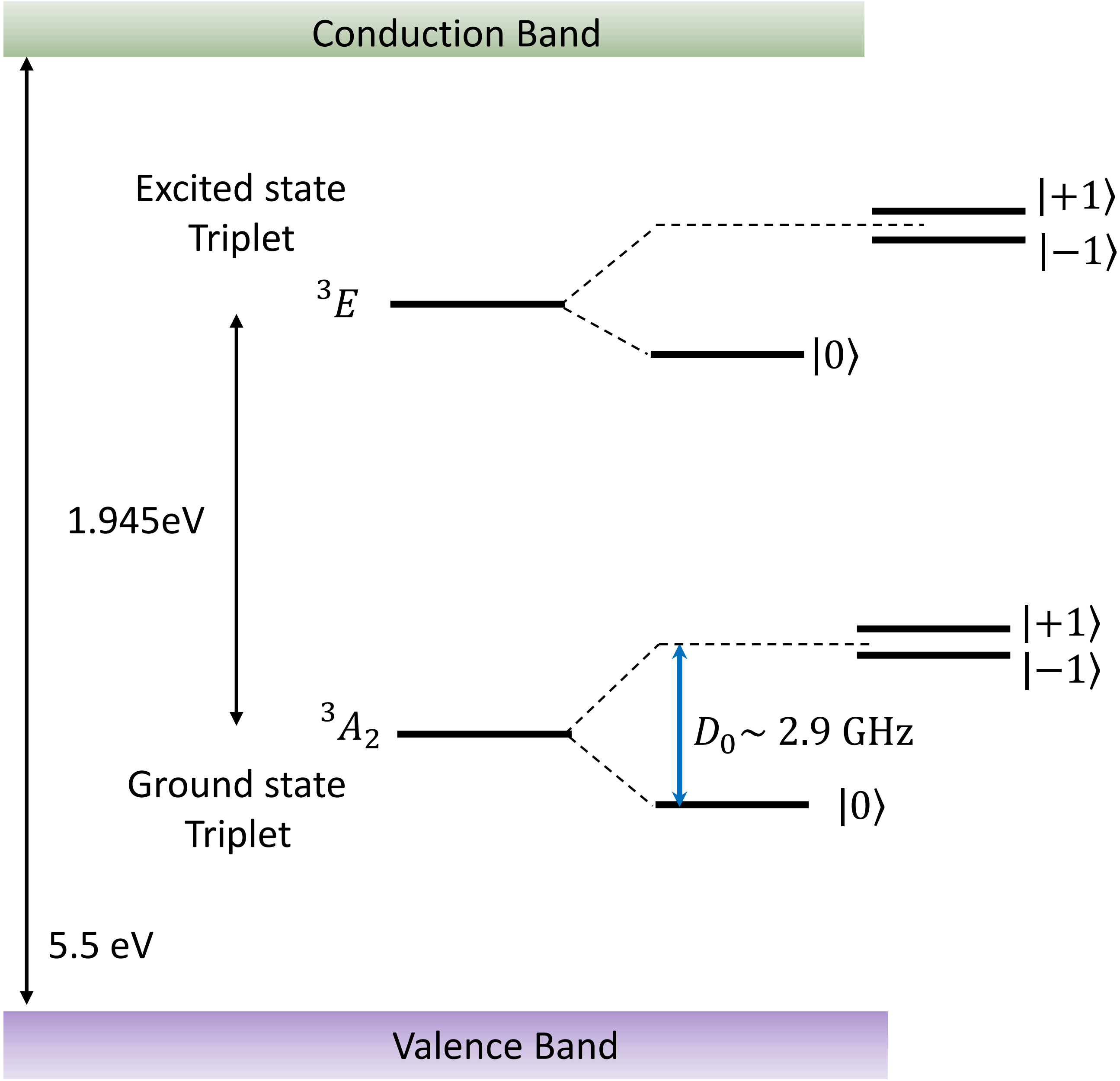

Electronic properties of the NV center

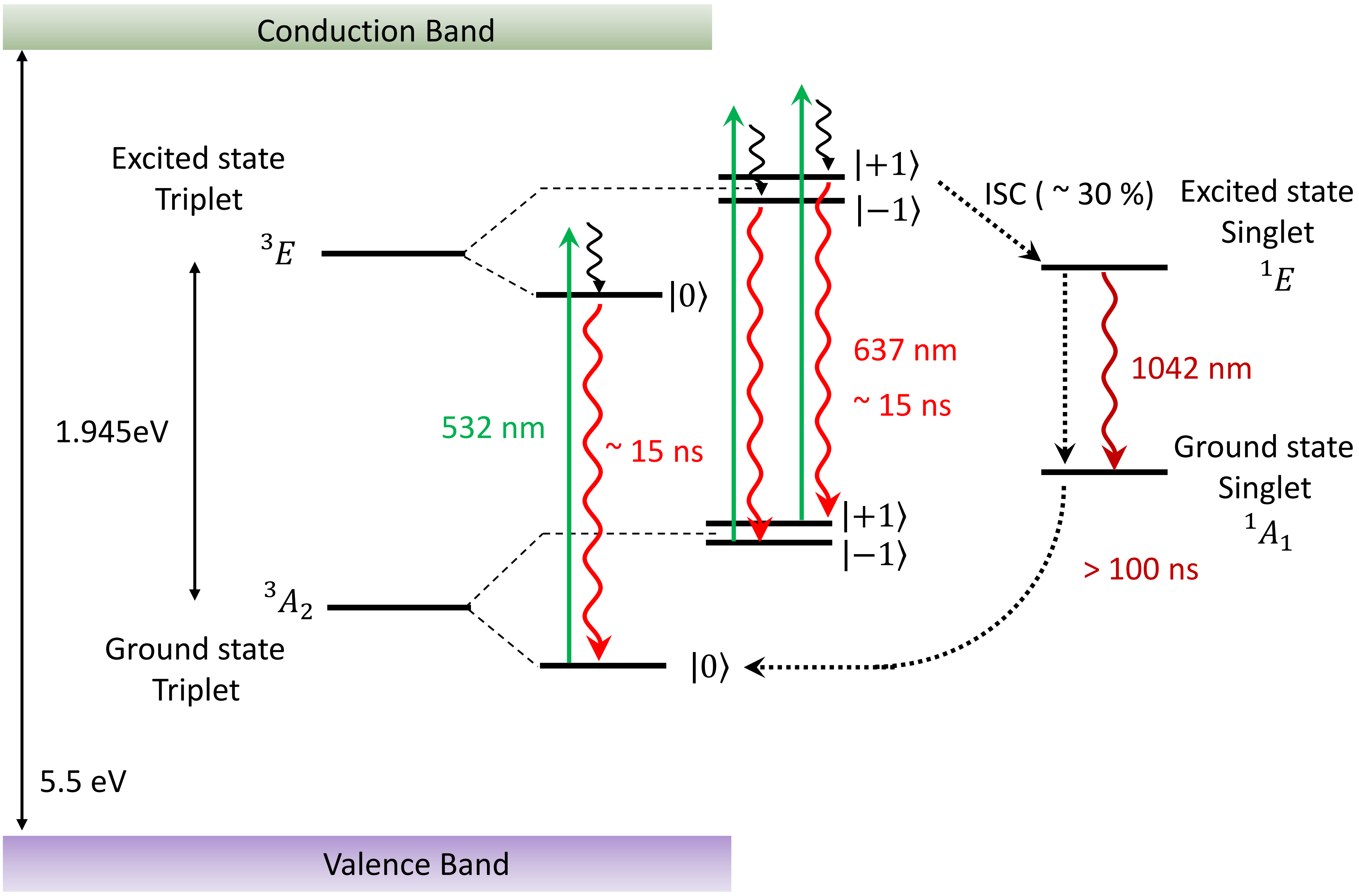

Electronic properties of the NV center

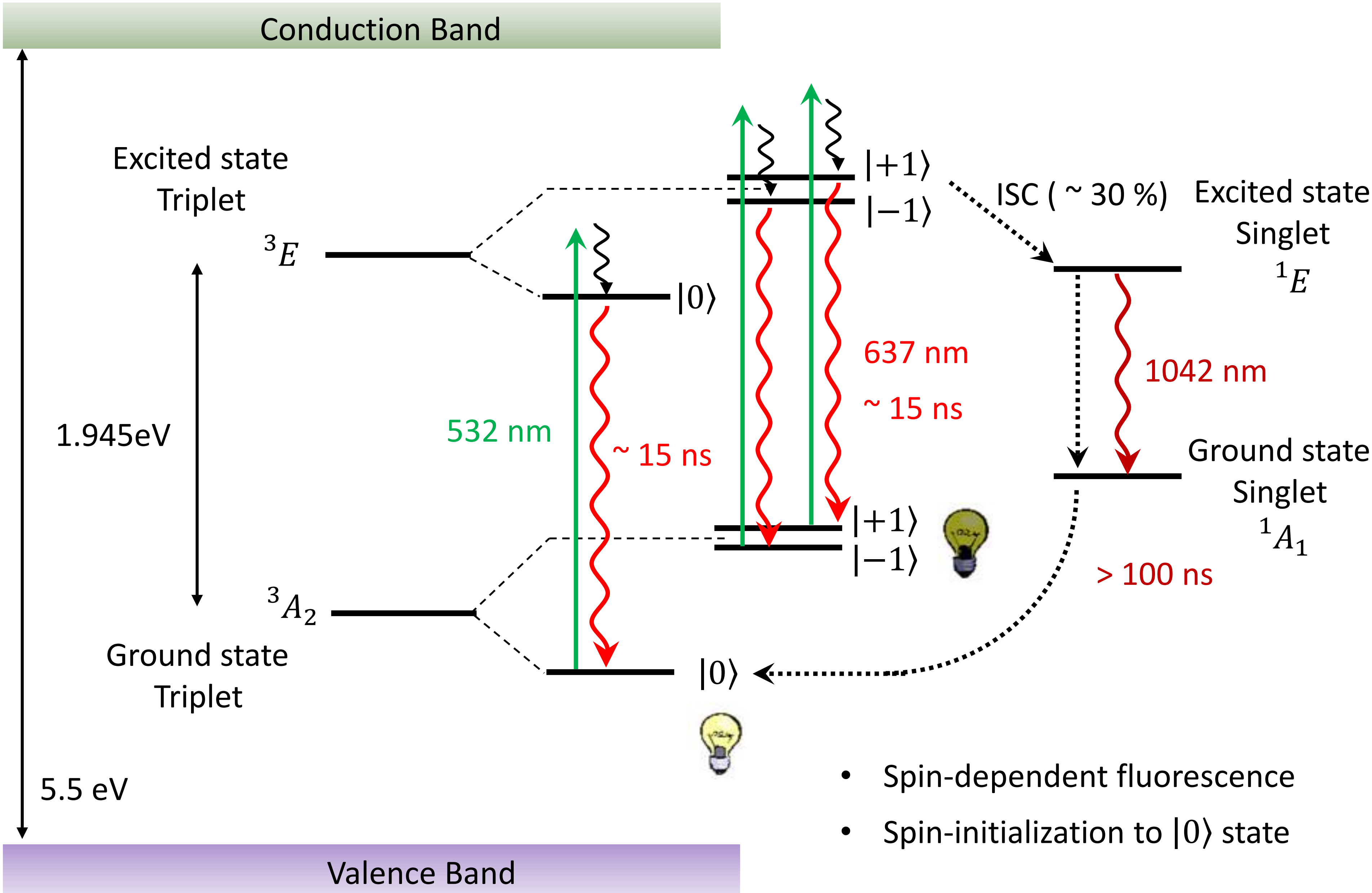

- Spin-dependent fluorescence
- Spin-initialization to $|0\rangle$ state

Electronic properties of the NV center

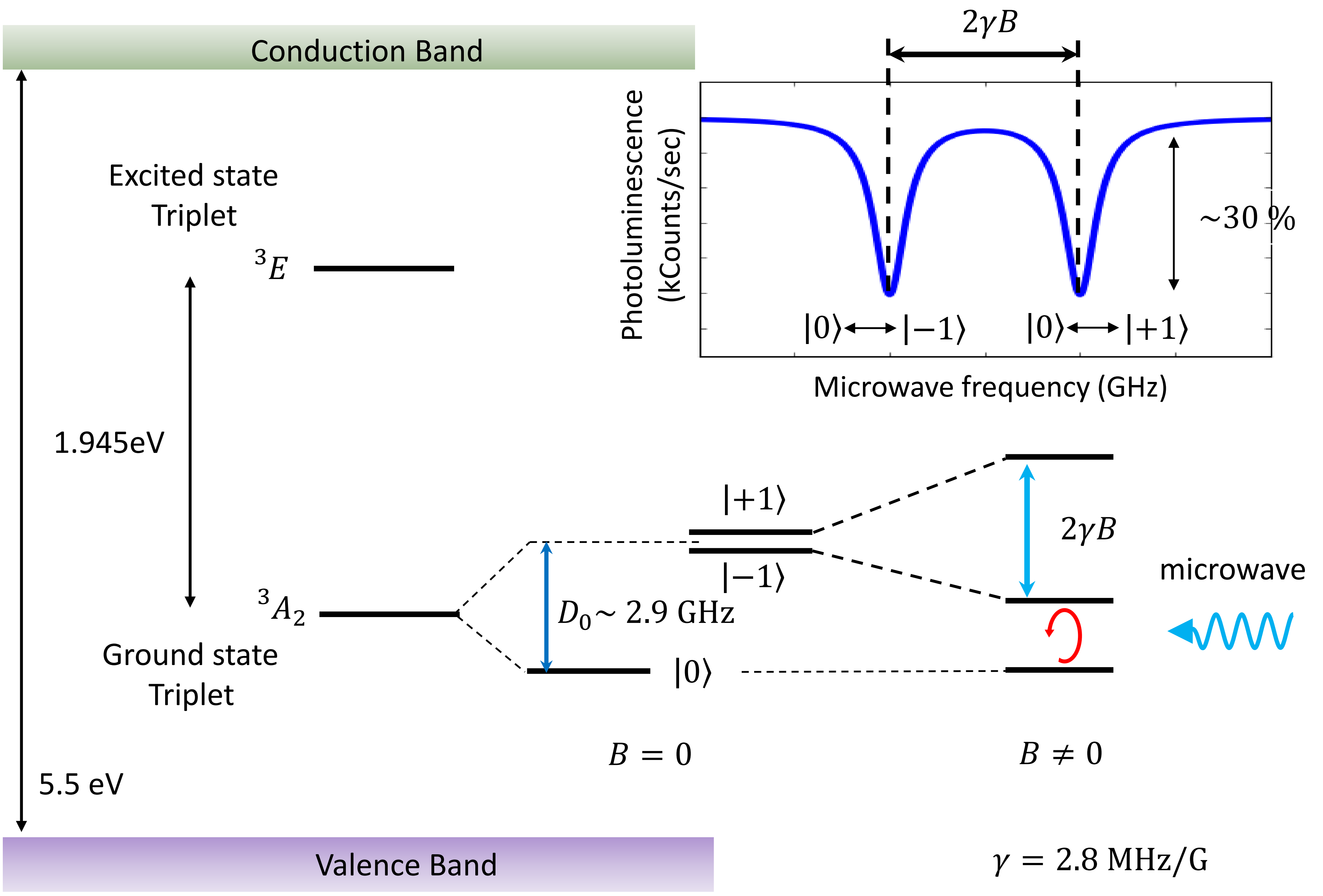

Electronic properties of the NV center

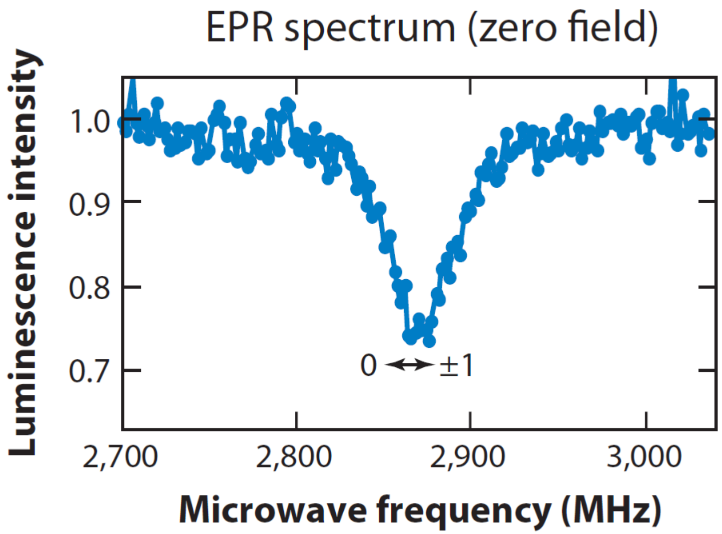

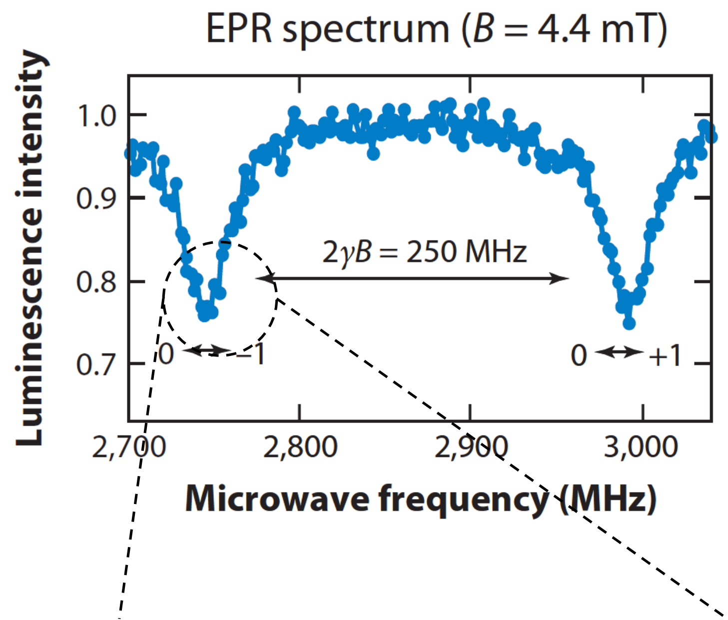

R. Schirhagl *et al.*, Annu. Rev. Phys. Chem. (2014)

Hyperfine interaction with ^{14}N (I = 1)

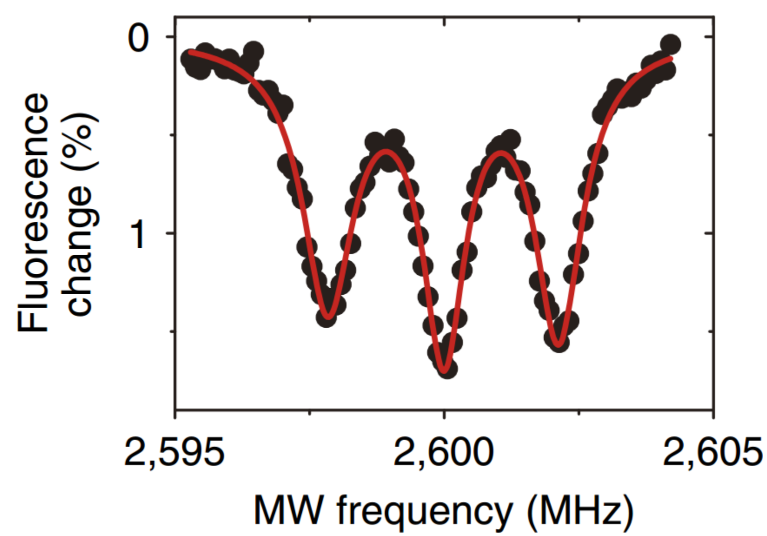

Ground-state Hamiltonian for NV center

zero-field splitting — Magnetic field — Hyperfine interaction

$$H = D_0 S_z^2 + \gamma \boldsymbol{S} \cdot \boldsymbol{B} + \boldsymbol{S} \cdot \boldsymbol{A_N} \cdot \boldsymbol{I_N}$$

$$+ d_z E_z S_z^2 + d_{xy}[E_x(S_x S_y + S_y S_x) + E_y(S_x^2 - S_y^2)$$

Electric or strain field

Outline

- Basics of the NV center
  - Structure, electronic, optical properties
  - Spin physics, coherence properties
- Applications for quantum metrology
  - Magnetic field sensing
  - Strain field sensing

Spin physics and coherence properties of the NV center

- T_1 : spin-lattice relaxation time measured by population decay
- T_2 : spin-spin dephasing time measured by Hahn echo or decoupling sequences
- T_2^*: inhomogeneous dephasing time measured by free induction decay

Rabi nutations

e.g. $|0\rangle \leftrightarrow |-1\rangle$ spin transition

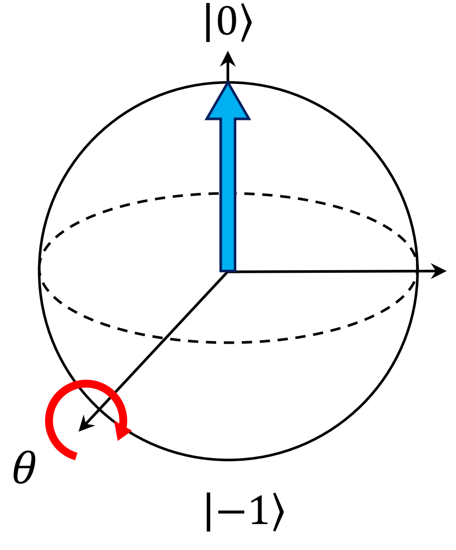

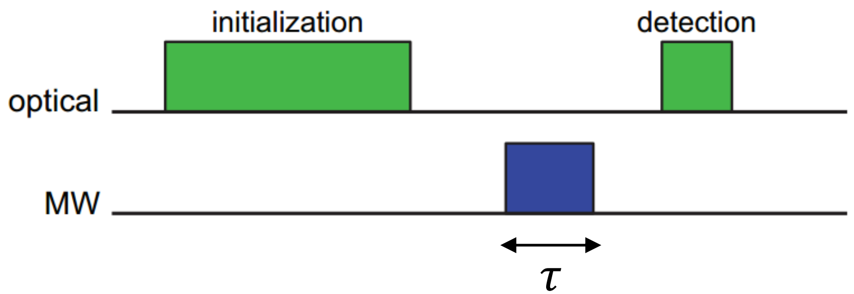

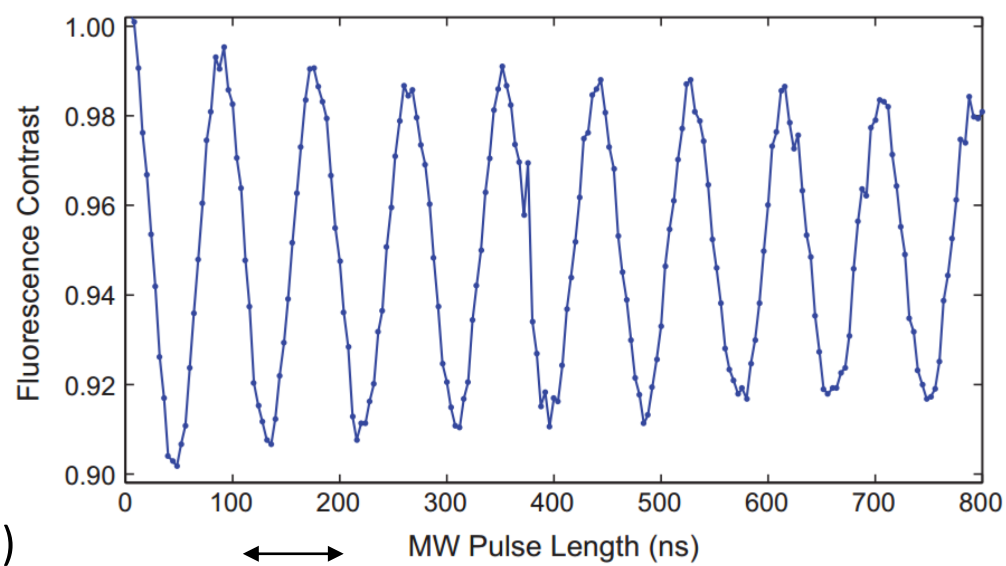

e.g. $\theta = \pi$ (π pulse), $\theta = \pi/2$ ($\pi/2$ pulse)

Rabi frequency : $\Omega \propto \sqrt{I_{MW}}$

Spin physics and coherence properties of the NV center

- T_1 : spin-lattice relaxation time measured by population decay

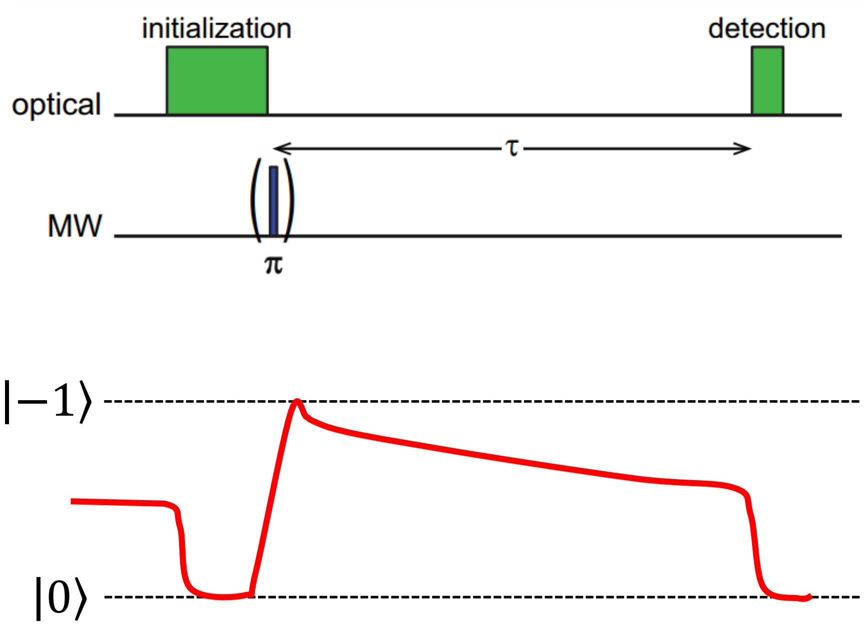

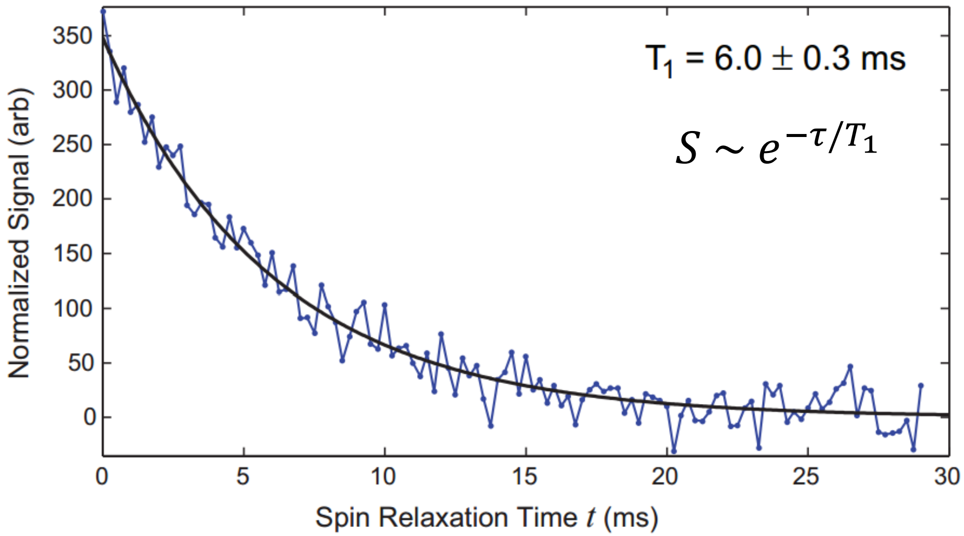

L. M. Pham, Ph. D. thesis (2013)

Spin physics and coherence properties of the NV center

- T_2^*: inhomogeneous dephasing time measured by Ramsey sequences

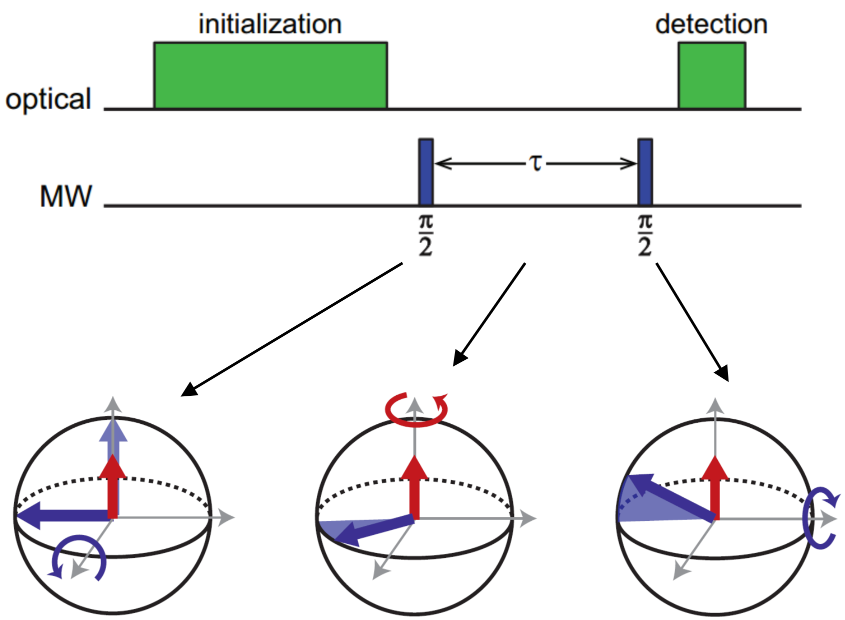

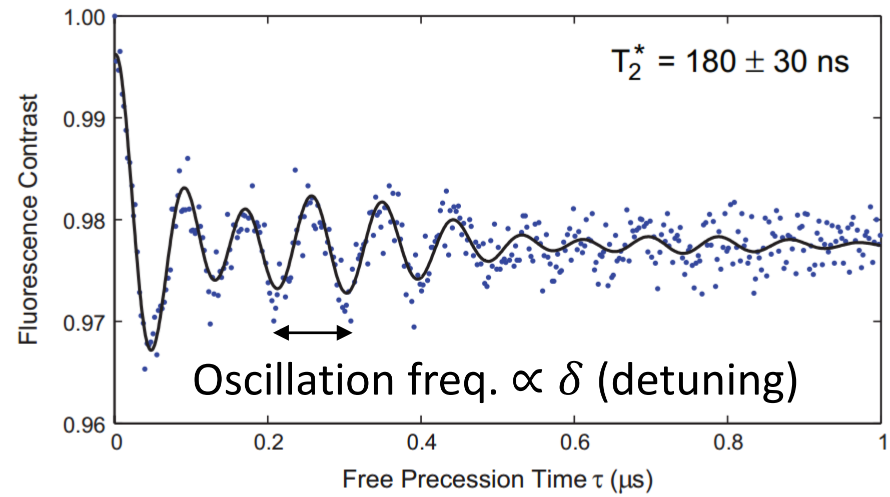

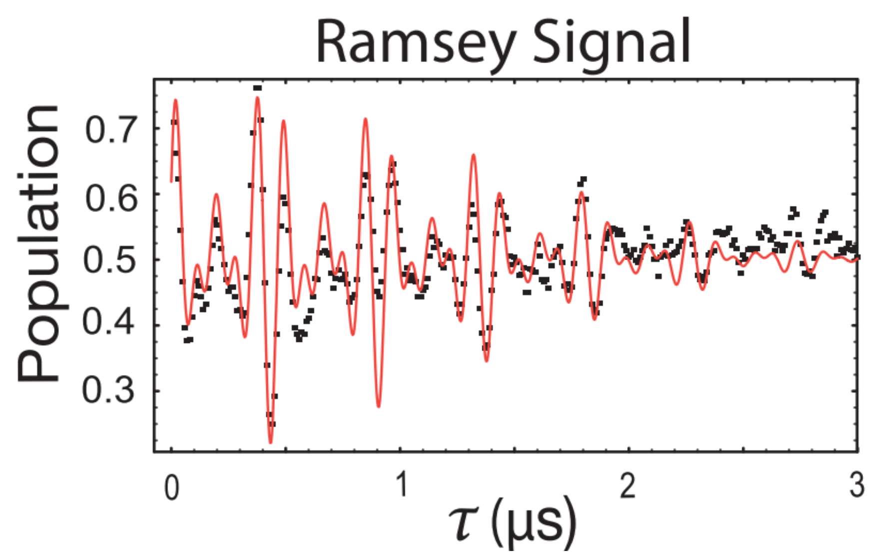

L. Childress *et al.*, Science (2006)

Spin physics and coherence properties of the NV center

- T_2 : spin-spin dephasing time measured by Hahn echo or decoupling sequences

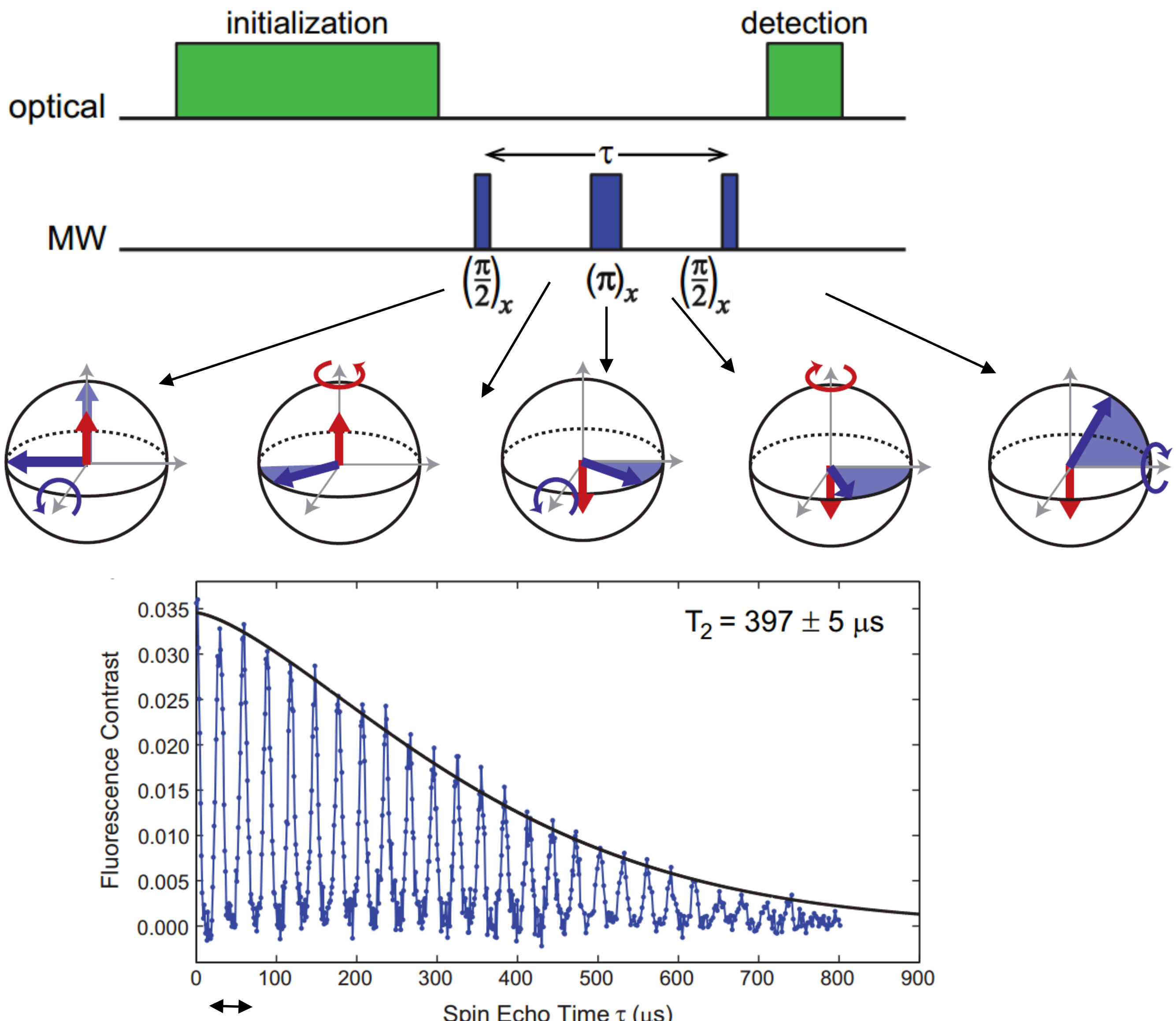

Larmor precession of ^{13}C nuclear spins (I = 1/2)

Unique properties of the NV center

- Spin qubits (or artificial atoms) in sold-state material
  (e.g. wide band gap, low spin-orbit coupling, large Debye temperature)
- Atomic-scale defect for high spatial resolution imaging
- Optical initialization and readout of spin state
- Long coherence times at even room temperature (T_2 > ms)
- Fast spin control and qubit gates (~ ns)
- Operates from cryogenic temperatures to ambient
- Chemically stable, non-toxic and bio-friendly
- Optically stable (free from photobleaching)
- High field sensitivity e.g. magnetic, electric, strain field, temperature

Property	Sensitivity	Property	Sensitivity
Magnetic field	**< 1 $nT/Hz^{1/2}$**	**Strain field**	**< $10^{-7}/Hz^{1/2}$**
Electric field	**< 100 $Vcm^{-1}/Hz^{1/2}$**	**Temperature**	**< 0.1 $K/Hz^{1/2}$**

Outline

- Basics of the NV center
  - Structure, electronic, optical properties
  - Spin physics, coherence properties
- Applications for quantum metrology
  - Magnetic field sensing
  - Strain field sensing

Magnetic field sensing with high sensitivity and high spatial resolution

Magnetic information

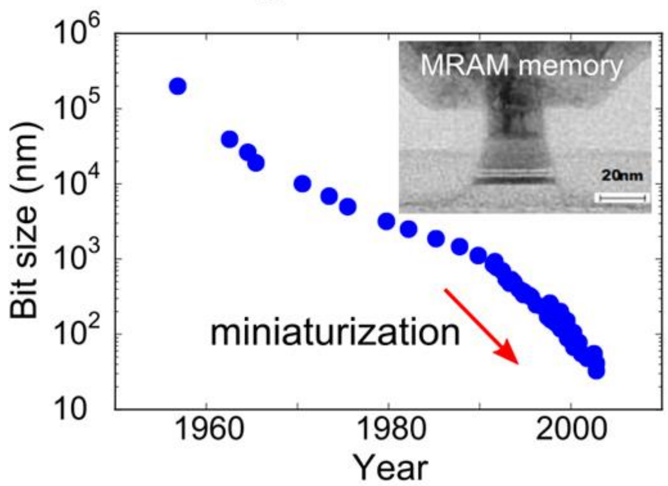

Skyrmion

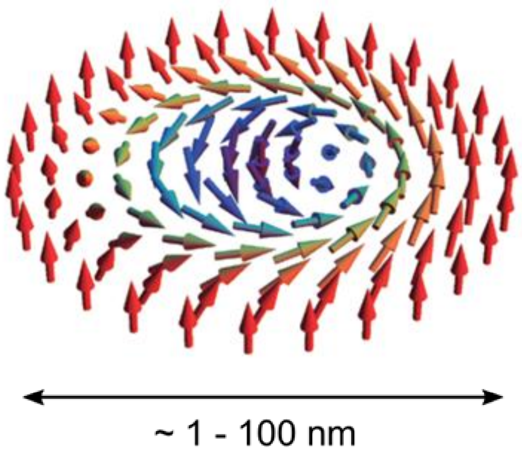

Biomedicne

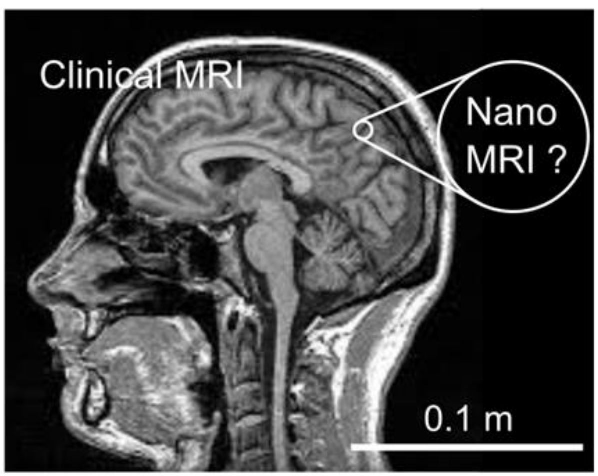

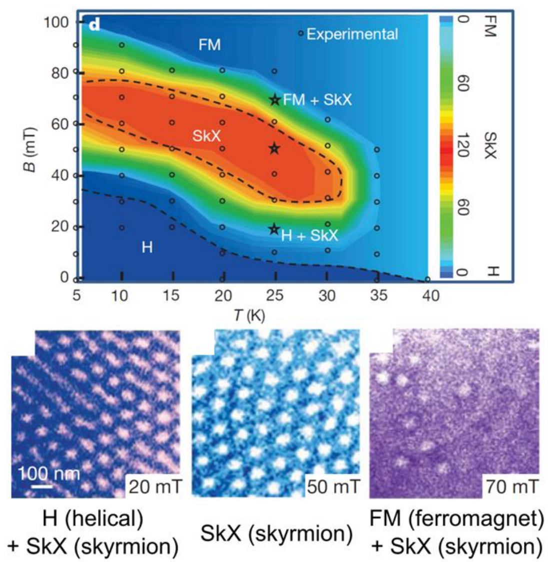

Magnetic field sensing: detecting schemes of DC field

CW ESR method

Pulsed ESR method
e.g. Ramsey sequences

T_1 relaxometry

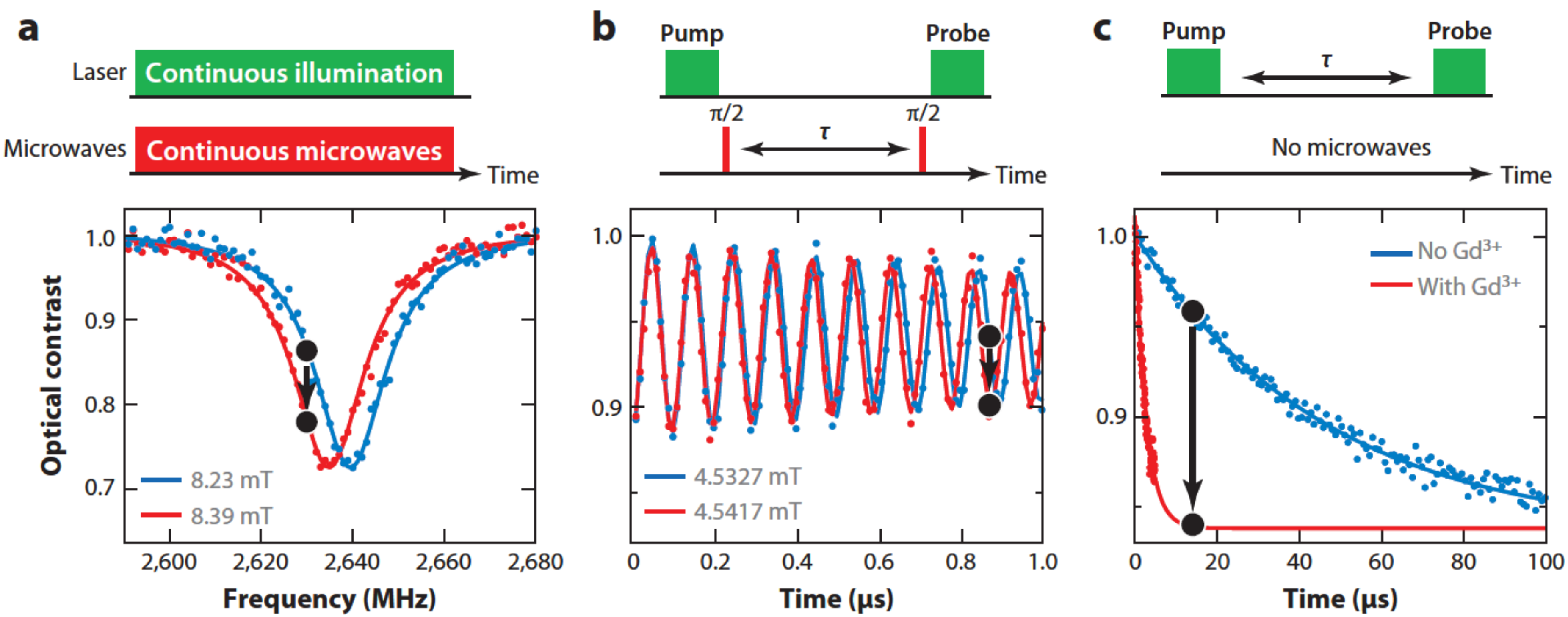

Oscillation frequency

$\propto \delta$ (detuning)

R. Schirhagl *et al.*, Annu. Rev. Phys. Chem. (2014)

Magnetic field sensing: detecting schemes of DC field

CW ESR method

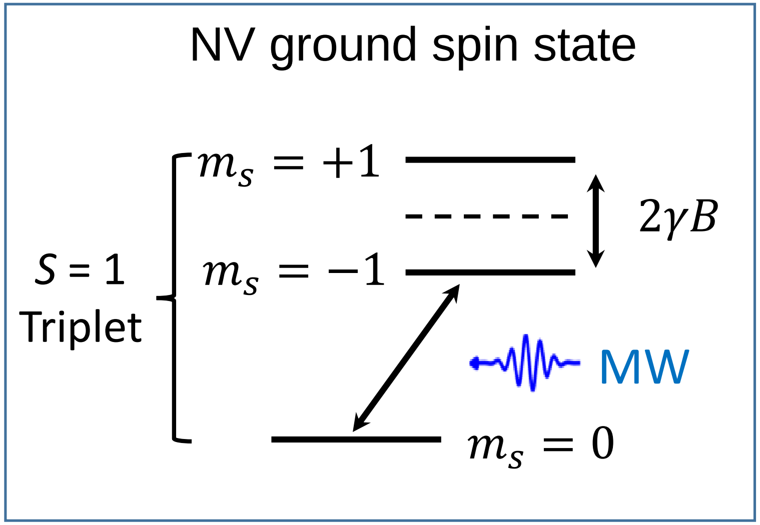

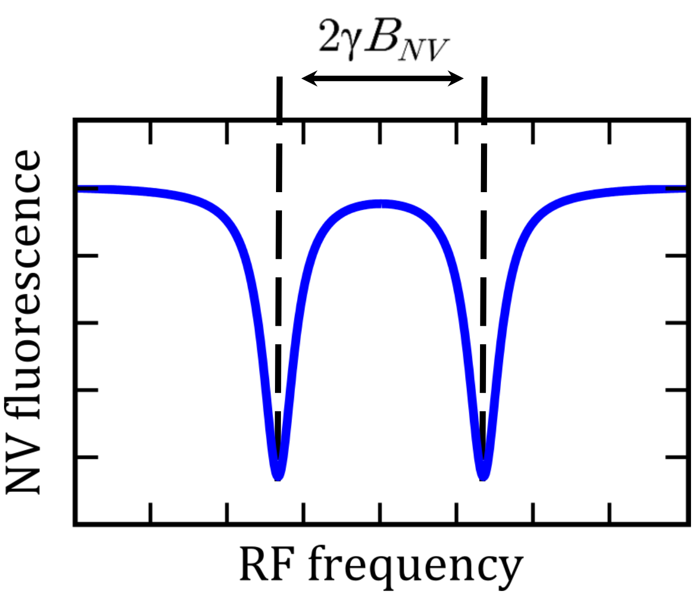

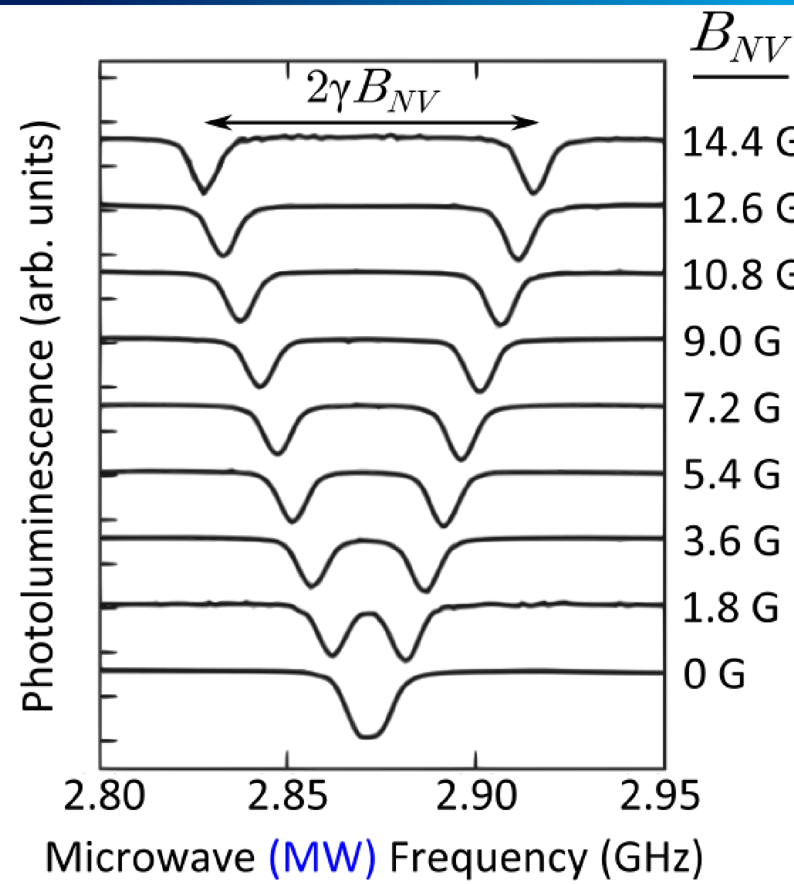

$$\eta_{DC} = \delta B_{min}\sqrt{t} \approx \frac{\Delta f \sqrt{t}}{\gamma C \sqrt{I_0}}$$

- measurement time: t
- linewidth: Δf
- $\gamma \simeq 2.8$ MHz/G
- $C \approx 20 - 30\%$
- Photon count rate: I_0

Example of DC field imaging with scanned probes

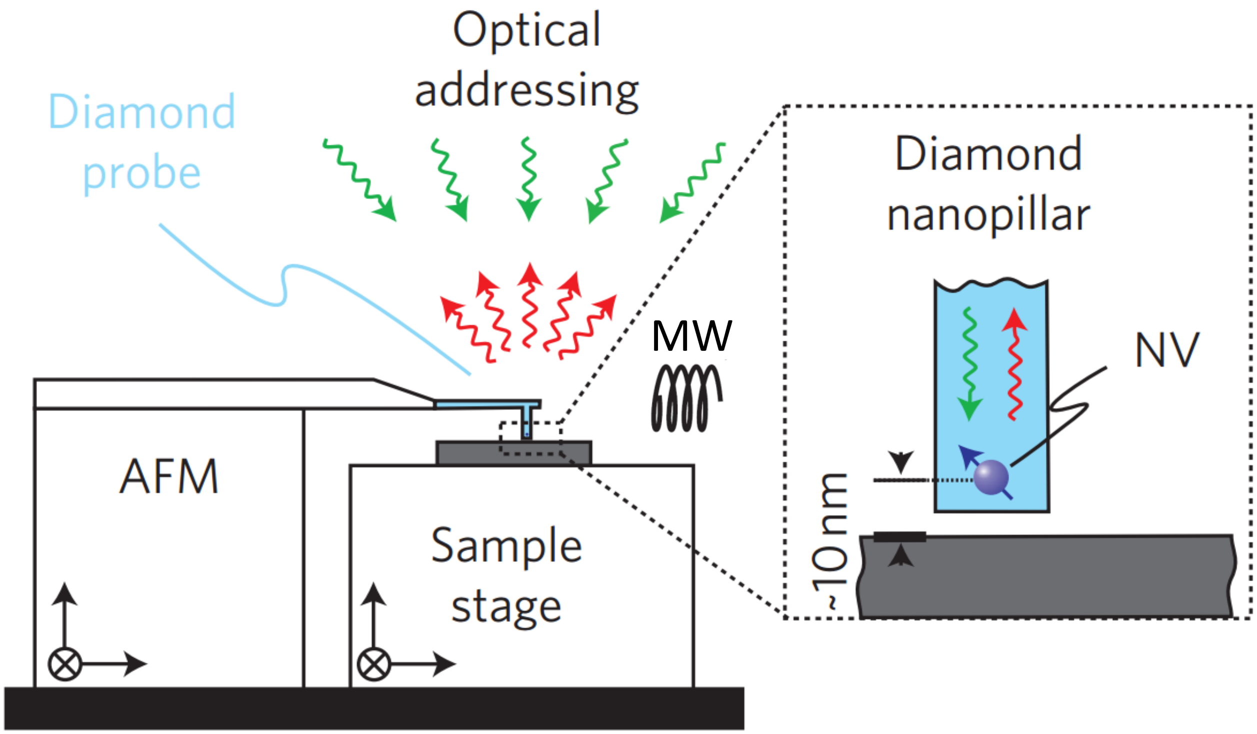

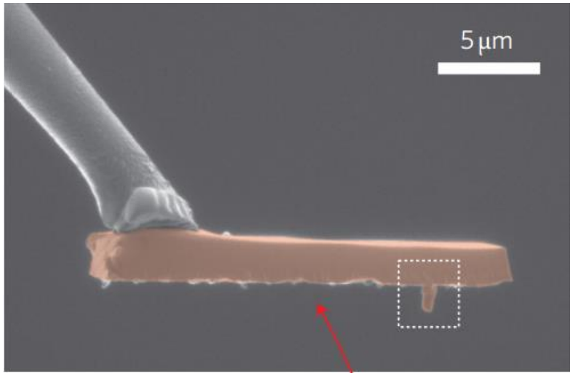

P. Malentinsky *et al.*, Nature Nanotechnology (2012)

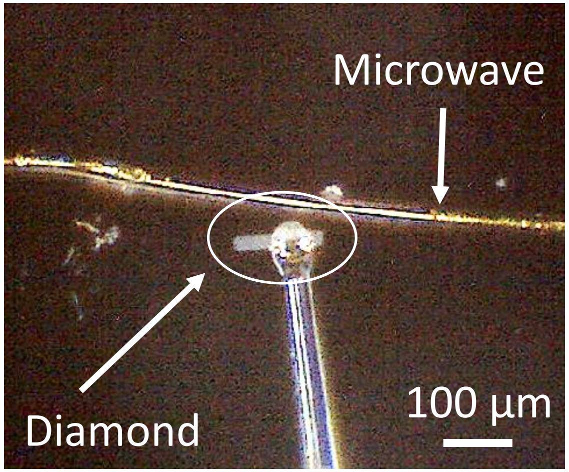

UCSB setup

Example of DC field imaging with scanned probes

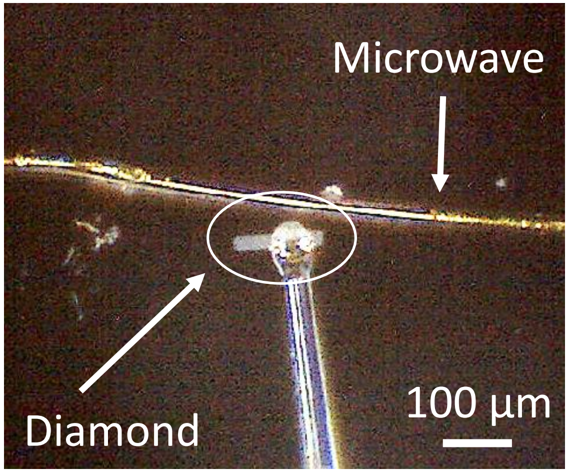

UCSB setup

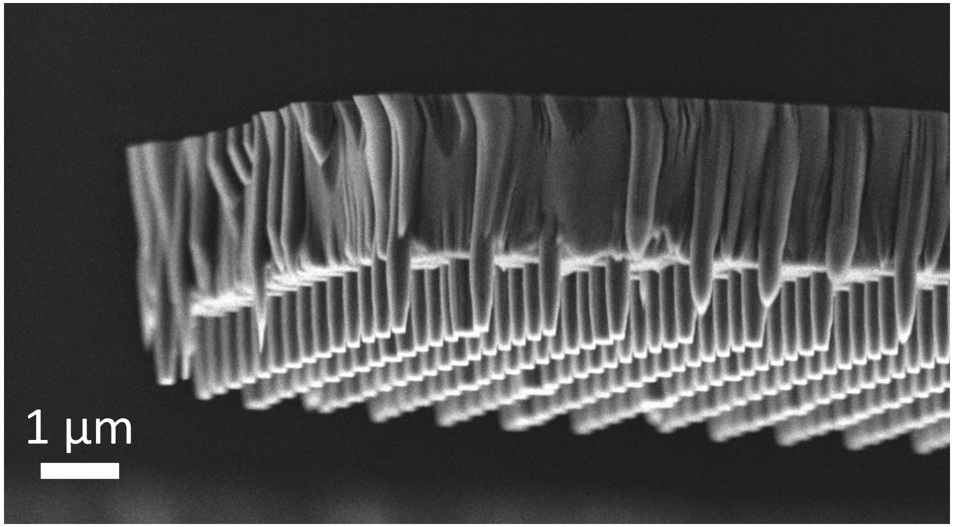

- Single crystal diamond cantilevers fabricated with pillars to aid in photon collection
- NV depth ~ 20 nm, on average 1 NV per pillar
- These cantilevers are then attached to custom tuning fork probes for force sensing

Confocal scan (30 µW @ 532 nm)

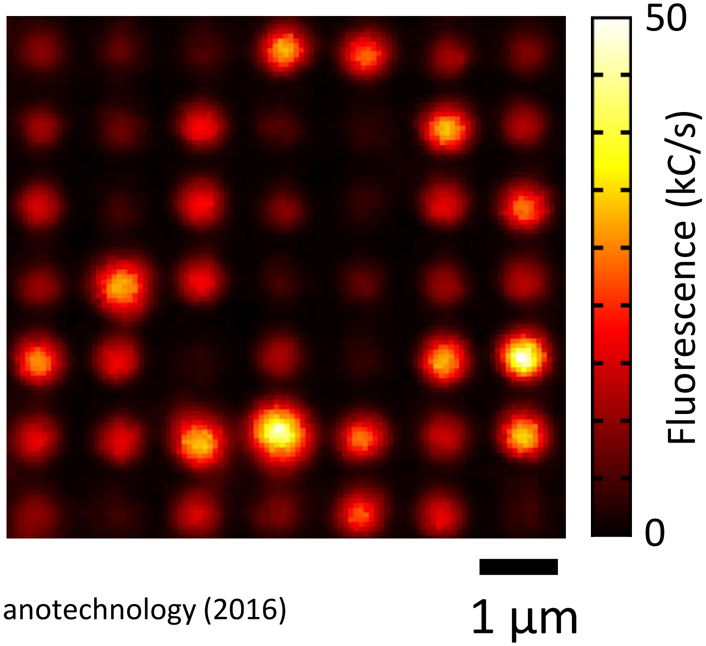

M. Pelliccione *et al.*, Nature Nanotechnology (2016)

Example of DC field imaging: hard disk

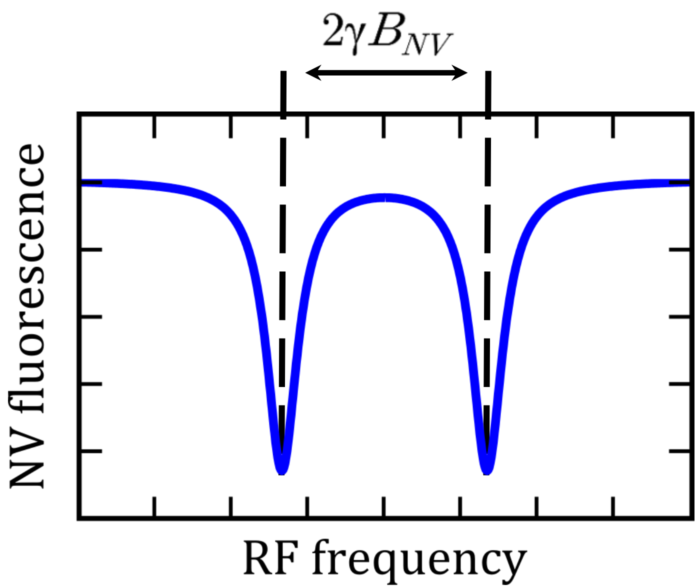

30 μW @ 532 nm
2 seconds per pixel

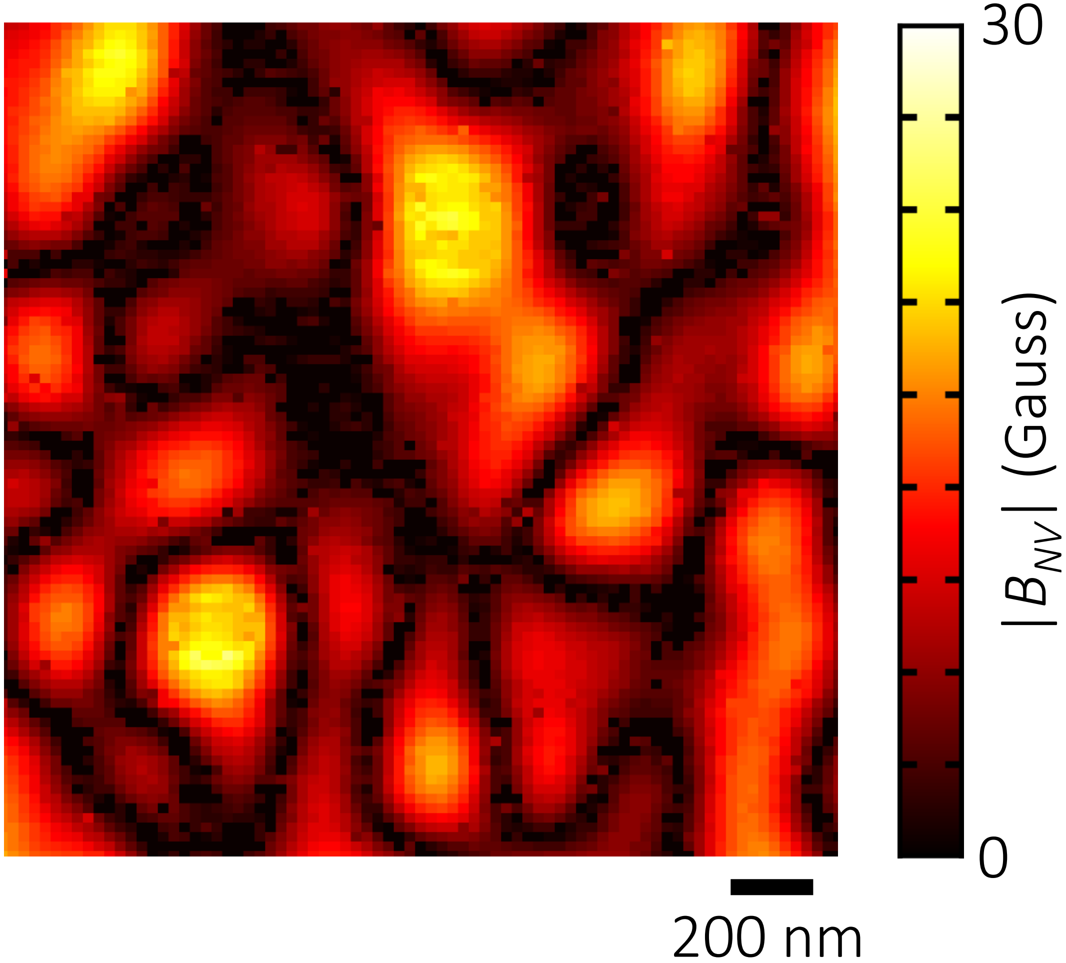

DC field sensitivity: 0.32 G/√Hz, dynamic range: 30 Gauss

From UCSB group
M. Pelliccione *et al.*, Nature Nanotechnology (2016)

Example of DC field imaging: hard disk

Alternate method: Use a fixed RF frequency to trace out magnetic field contours.

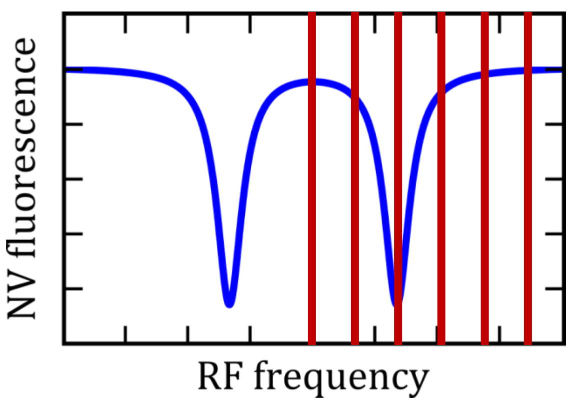

30 μW @ 532 nm
0.1 seconds per pixel
DC sensitivity: 0.03 G/√Hz
Dynamic range: 1 Gauss

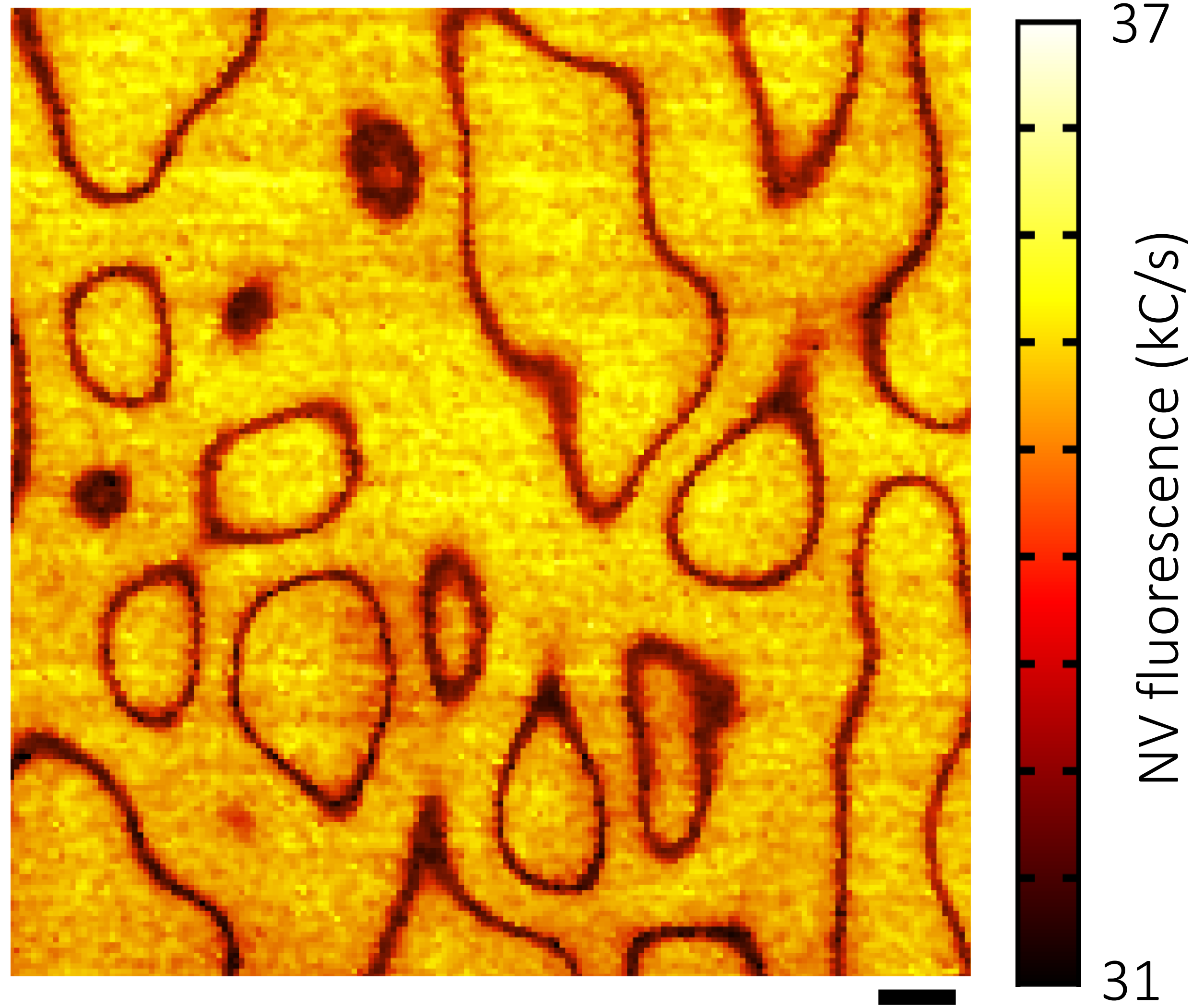

More examples of DC field imaging

Hard disk

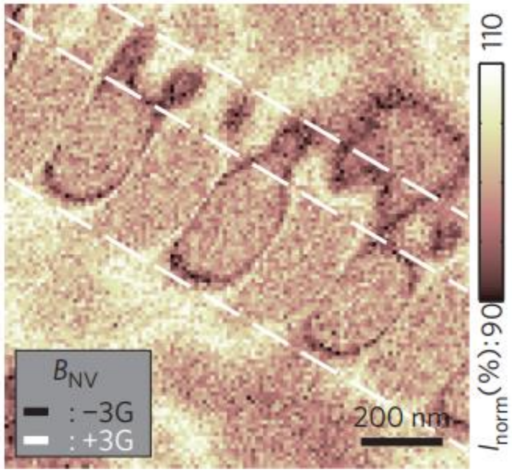

P. Malentinsky *et al.*, Nature Nanotechnology (2012)

Magnetic vortex

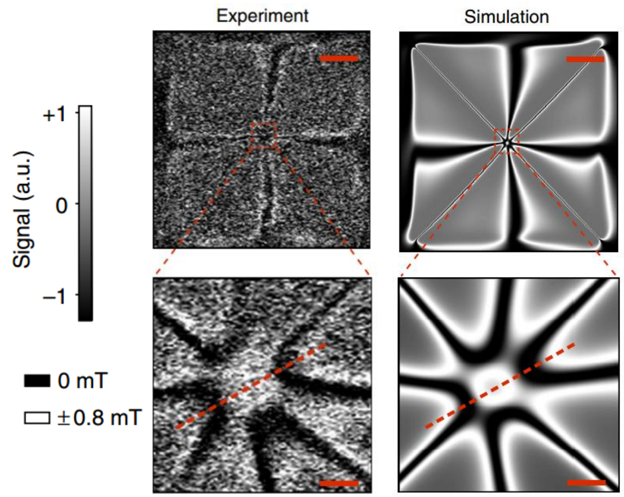

L. Rondin *et al.*, Nature Communications (2013)

Domain wall

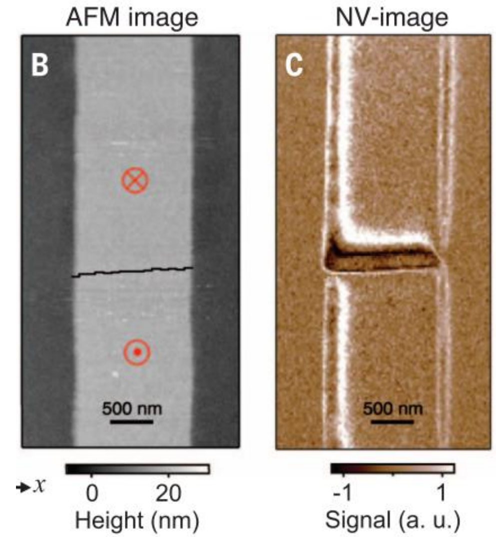

J. P. Tetienne *et al.*, Science (2014)

Superconducting vortices in $BaFe_2(As_{0.7}P_{0.3})_2$

T = 6 K

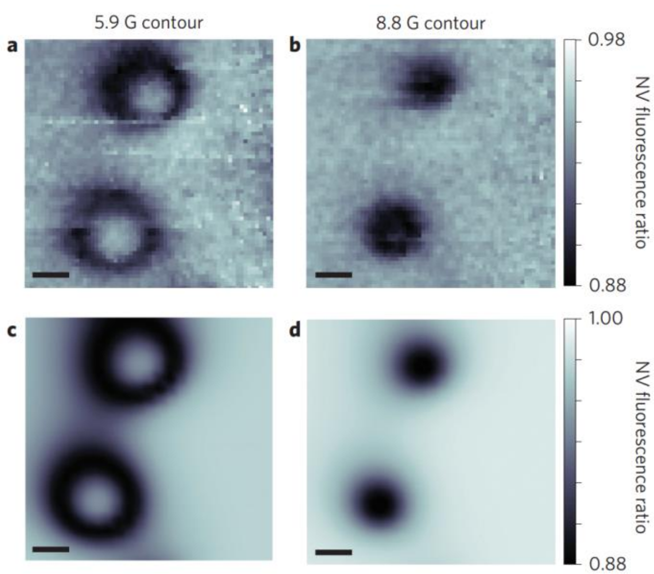

M. Pelliccione *et al.*, Nature Nanotechnology (2016)

Superconducting vortex in YBCO

T = 4.2 K

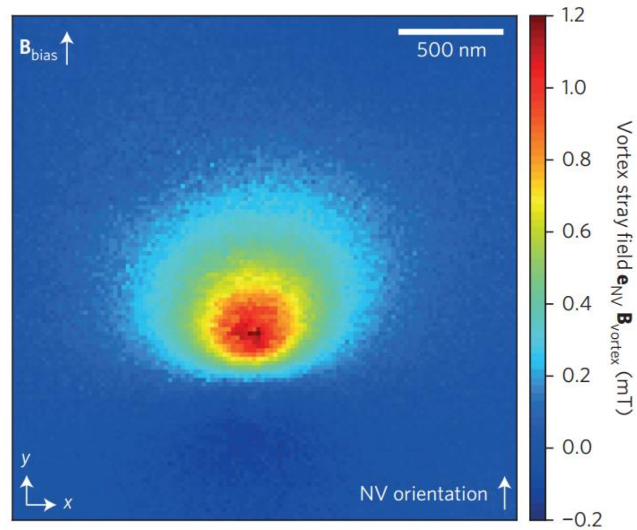

L. Thiel *et al.*, Nature Nanotechnology (2016)

Magnetic field sensing: detecting schemes of DC field

Pulsed ESR method e.g. Ramsey sequences $\frac{\pi}{2} - \tau - \frac{\pi}{2}$

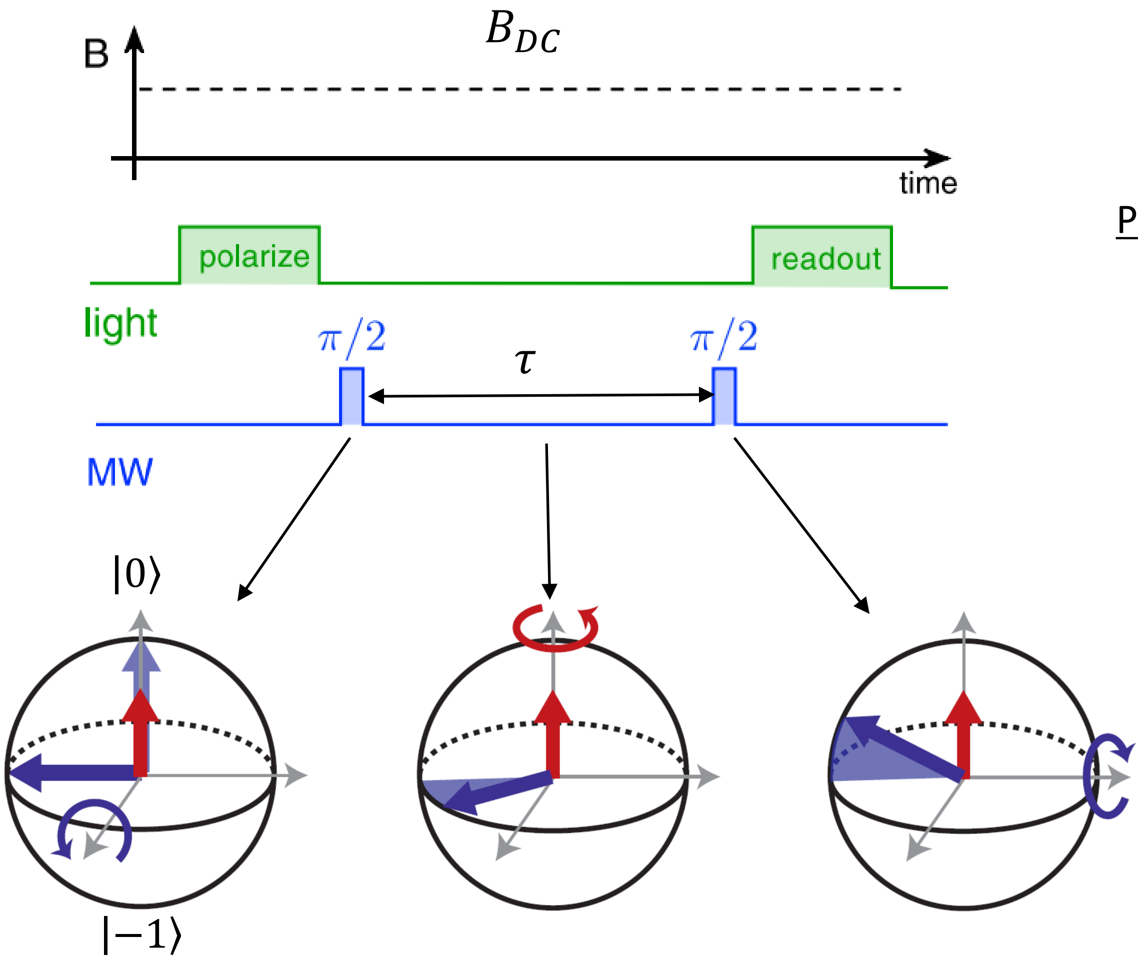

$|\psi\rangle = \frac{1}{\sqrt{2}}(|0\rangle + |-1\rangle)$

$|\psi\rangle = \frac{1}{\sqrt{2}}(|0\rangle + e^{i\phi}|-1\rangle)$

$\phi = \gamma B_{DC}\tau$

Photon shot-noise limited DC field sensitivity

$$\eta_{DC} \approx \frac{1}{\gamma}\frac{1}{C\sqrt{I_0}}\frac{1}{\sqrt{T_2^*}}$$

${T_2}^*$: inhomogeneous dephasing time

$$\eta_{DC} \sim 10\ \mathrm{nT}/\sqrt{\mathrm{Hz}}$$
$$({T_2}^* \sim 100\ \mu s)$$

L. Rondin *et al.*, Rep. Prog. Phys. (2014)
S. Hong *et al.*, MRS Bulletin (2013)

Magnetic field sensing: detecting schemes of DC field

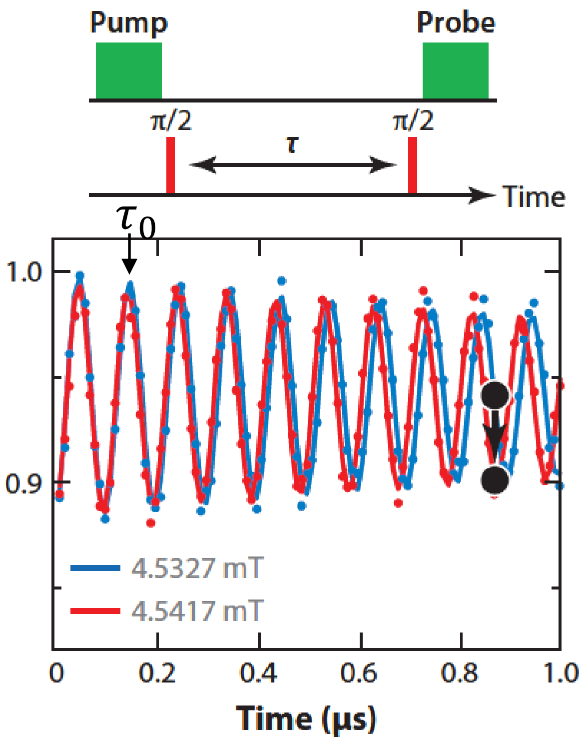

R. Schirhagl *et al.*, Annu. Rev. Phys. Chem. (2014)

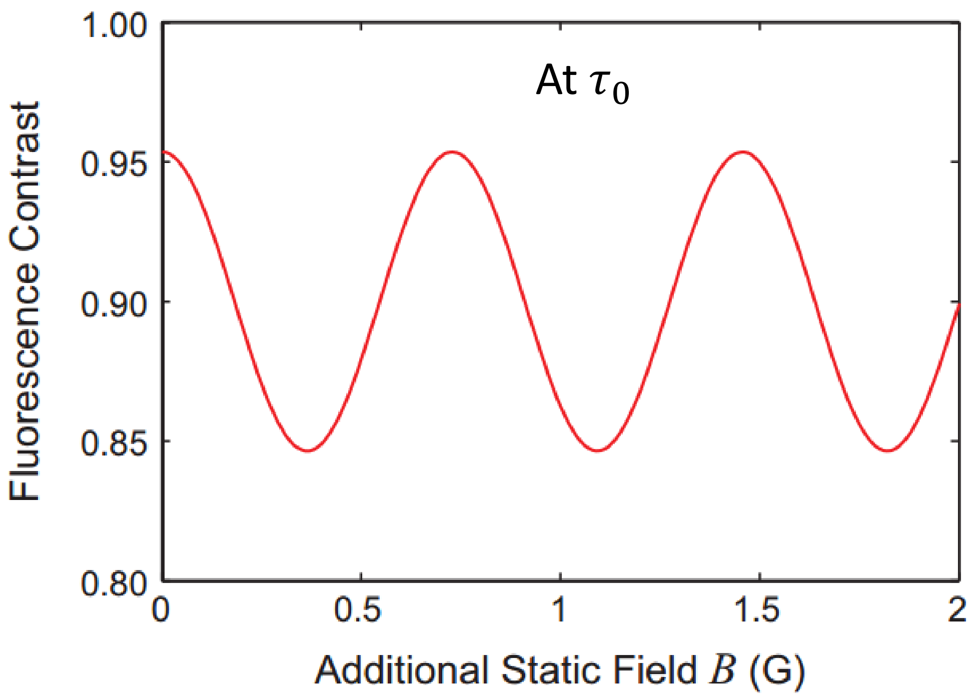

Photon signal :

$$S = \frac{a+b}{2} + \frac{a-b}{2}\cos(\phi) = \frac{a+b}{2} + \frac{a-b}{2}\cos(\gamma B_{DC}\tau)$$

a : number of photons at $\phi = 0$
b : number of photons at $\phi = \pi$

Magnetic field sensing: detecting schemes of AC field

Advanced pulse method   e.g. Hahn echo sequence $\frac{\pi}{2} - \tau - \pi - \tau - \frac{\pi}{2}$

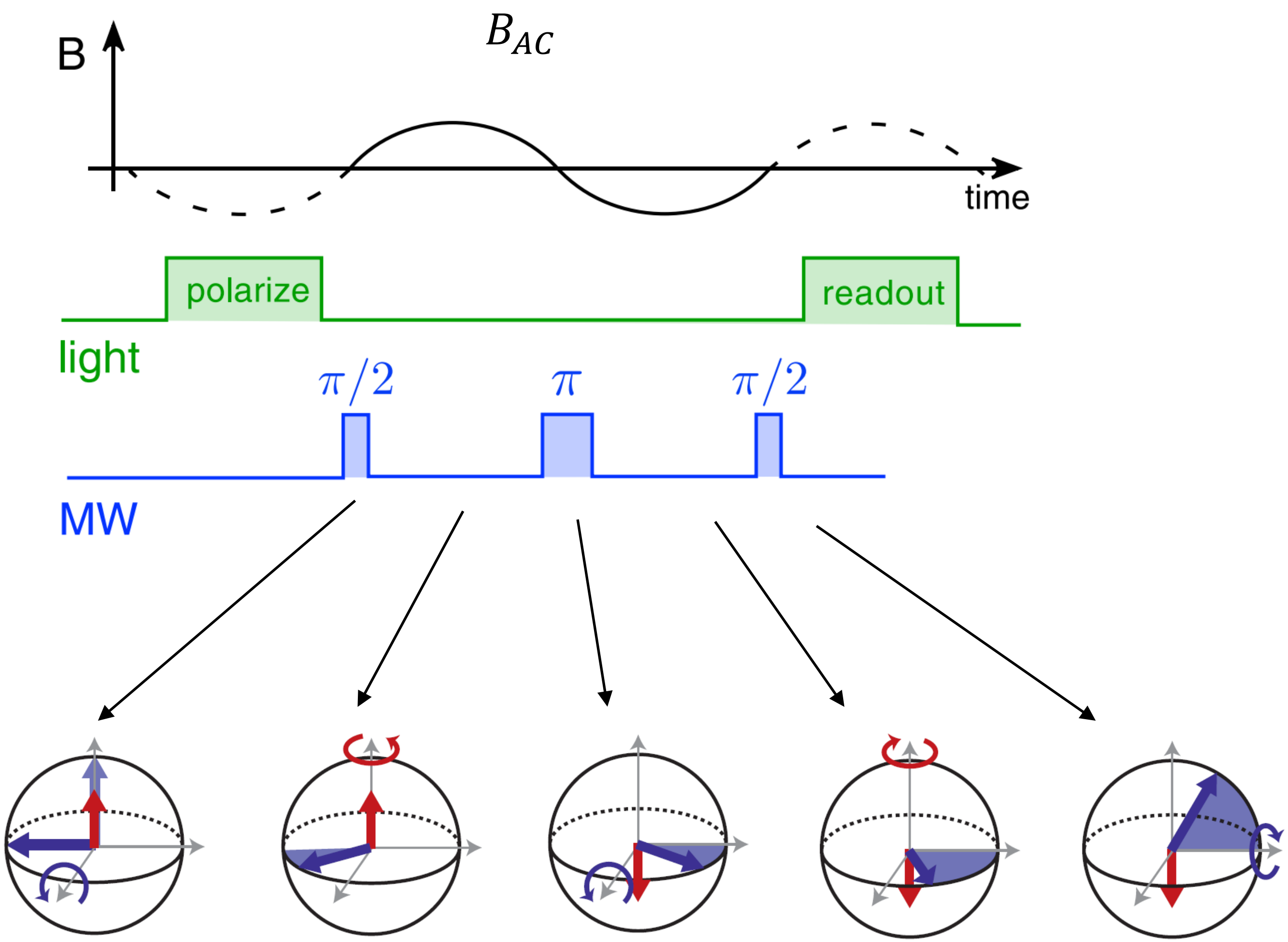

$\phi = 4\gamma B_{AC}\tau$

AC field sensitivity

$$\eta_{AC} \approx \frac{1}{\gamma}\frac{1}{C\sqrt{I_0}}\frac{1}{\sqrt{T_2}}$$

T_2 : dephasing time

$$\eta_{AC} \sim 1\ \mathrm{nT}/\sqrt{\mathrm{Hz}}$$
$$(T_2 \sim 1\ ms)$$

L. Rondin *et al.*, Rep. Prog. Phys. (2014)
S. Hong *et al.*, MRS Bulletin (2013)

Magnetic field sensing: detecting schemes of AC field

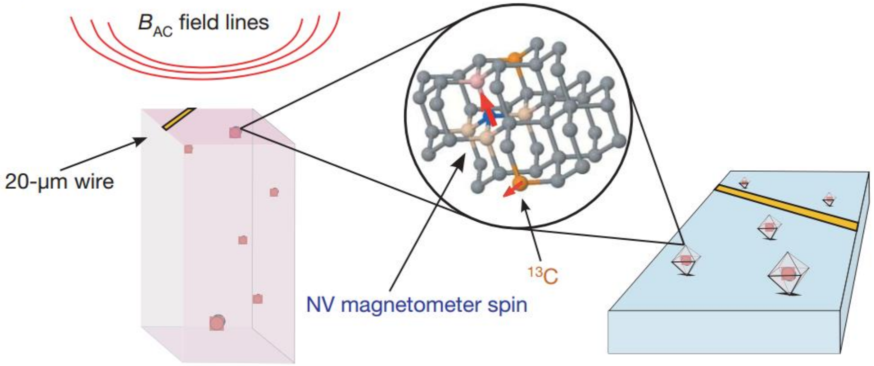

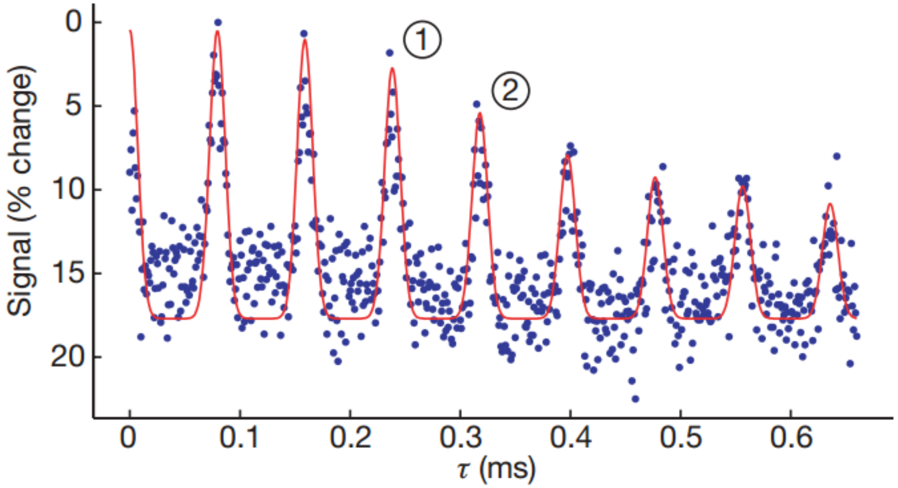

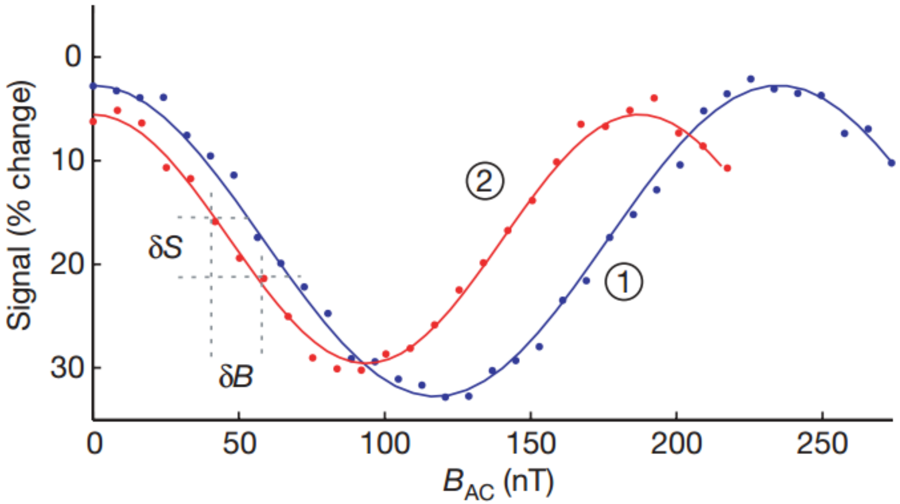

Photon signal :

$$S = \frac{a+b}{2} + \frac{a-b}{2}\cos(\phi) = \frac{a+b}{2} + \frac{a-b}{2}\cos(4\gamma B_{AC}\tau)$$

a : number of photons at $\phi = 0$
b : number of photons at $\phi = \pi$

$$\eta_{AC} \sim 30\ \mathrm{nT}/\sqrt{\mathrm{Hz}}$$

J. R. Maze *et al.*, Nature (2008)

Outline

- Basics of the NV center
  - Structure, electronic, optical properties
  - Spin physics, coherence properties
- Applications for quantum metrology
  - Magnetic field sensing
  - Strain field sensing

Strain field sensing with high sensitivity

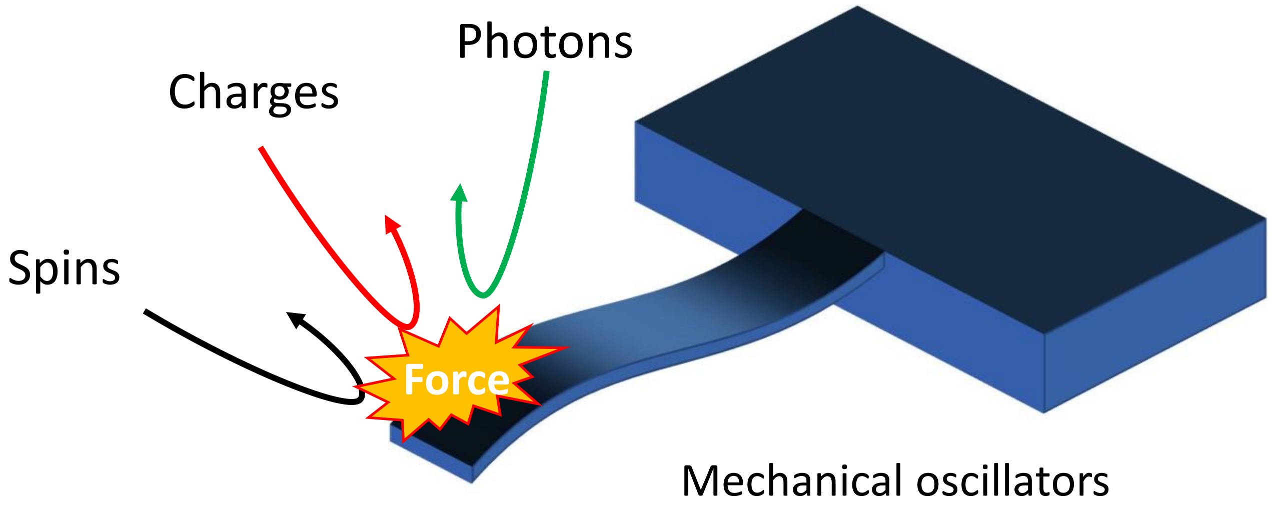

- Quantum sensors for force, mass, displacement, acceleration…
- Universal interface in quantum networks
- Quantum measurements in macroscopic mechanical object

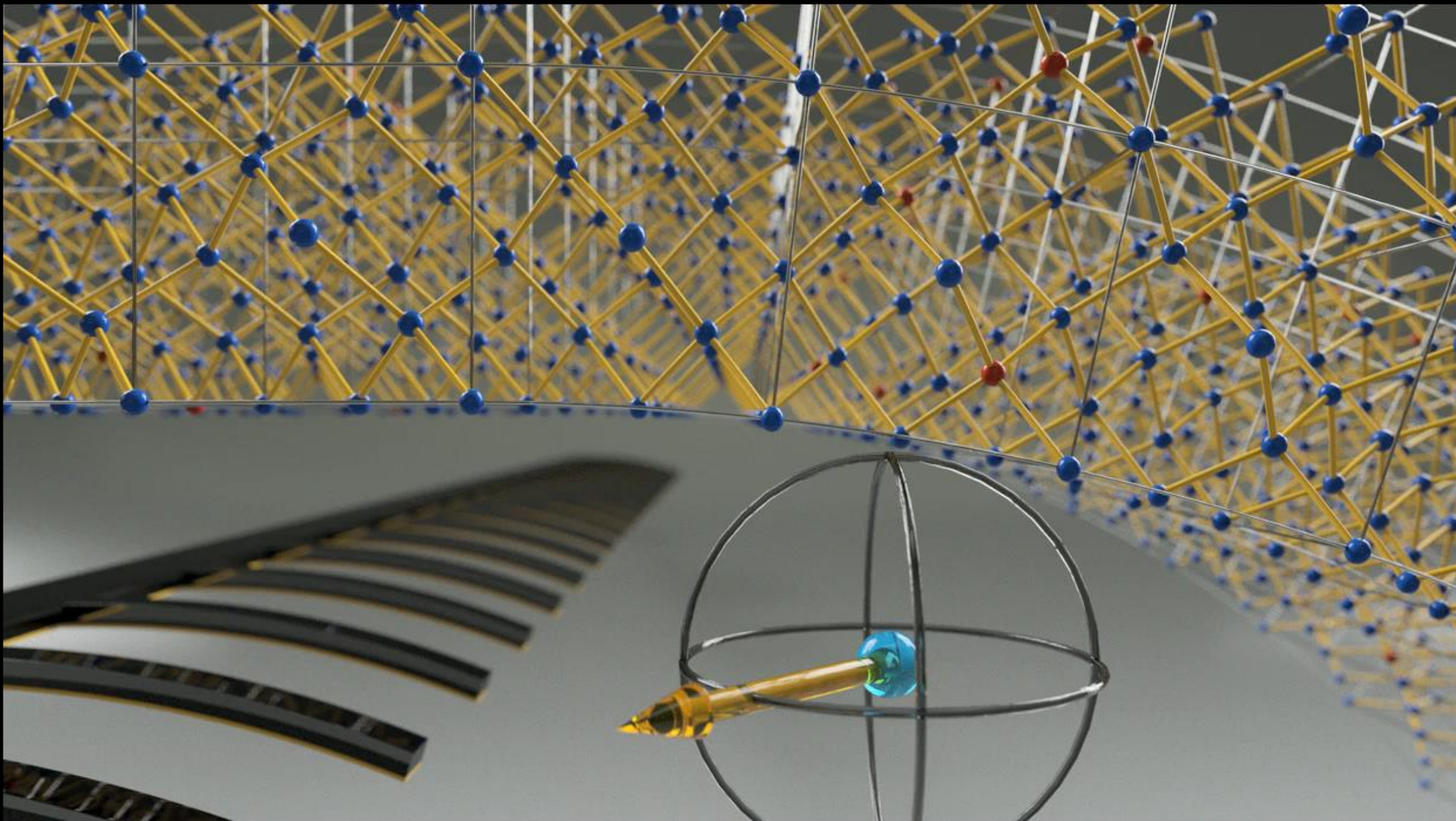

Strain field sensing

- Simulated stress profile of our cantilever (COMSOL)
- $60\ \mu m \times 15\ \mu m \times 1.1\ \mu m$, NV depth = 51.5 nm
- Fundamental flexural mode, $f_m = 882$ kHz
- Drive motion with a piezo actuator

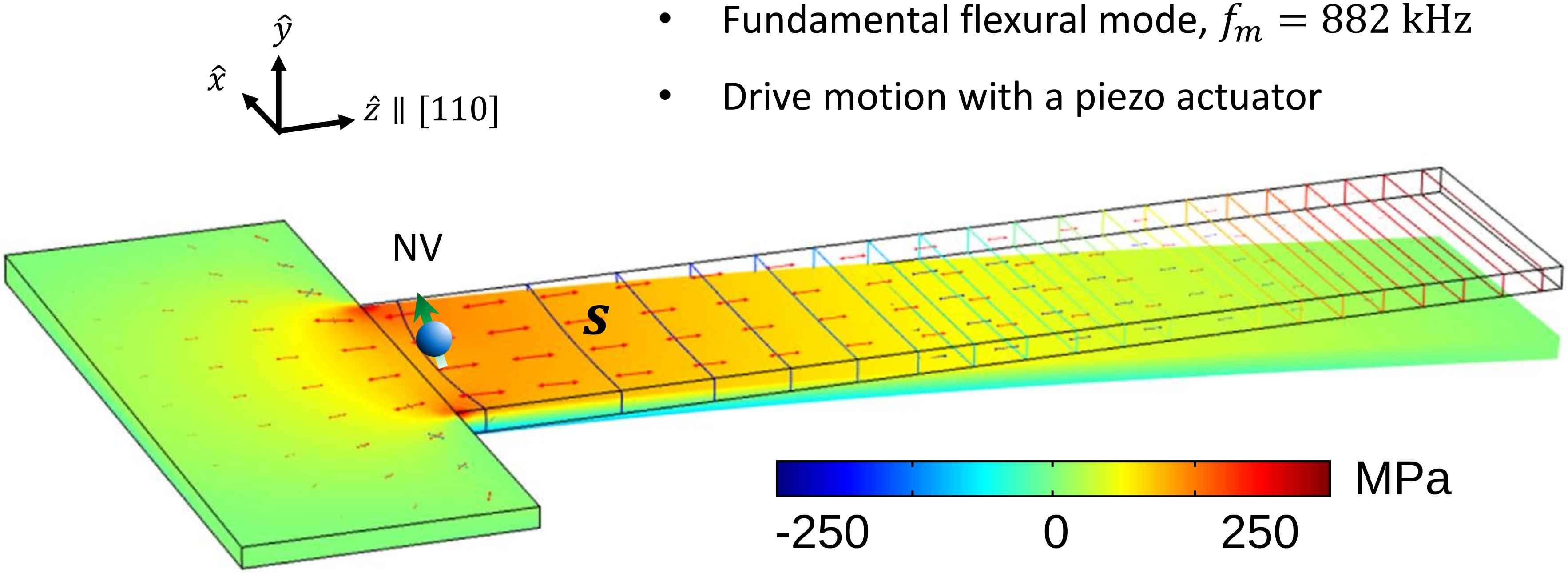

Strain tensor

$$\varepsilon = \begin{pmatrix} -\nu s & 0 & 0 \\ 0 & -\nu s & 0 \\ 0 & 0 & s \end{pmatrix}$$

s : strain along cantilever axis
ν : Poisson ratio, 0.11

Strain field sensing

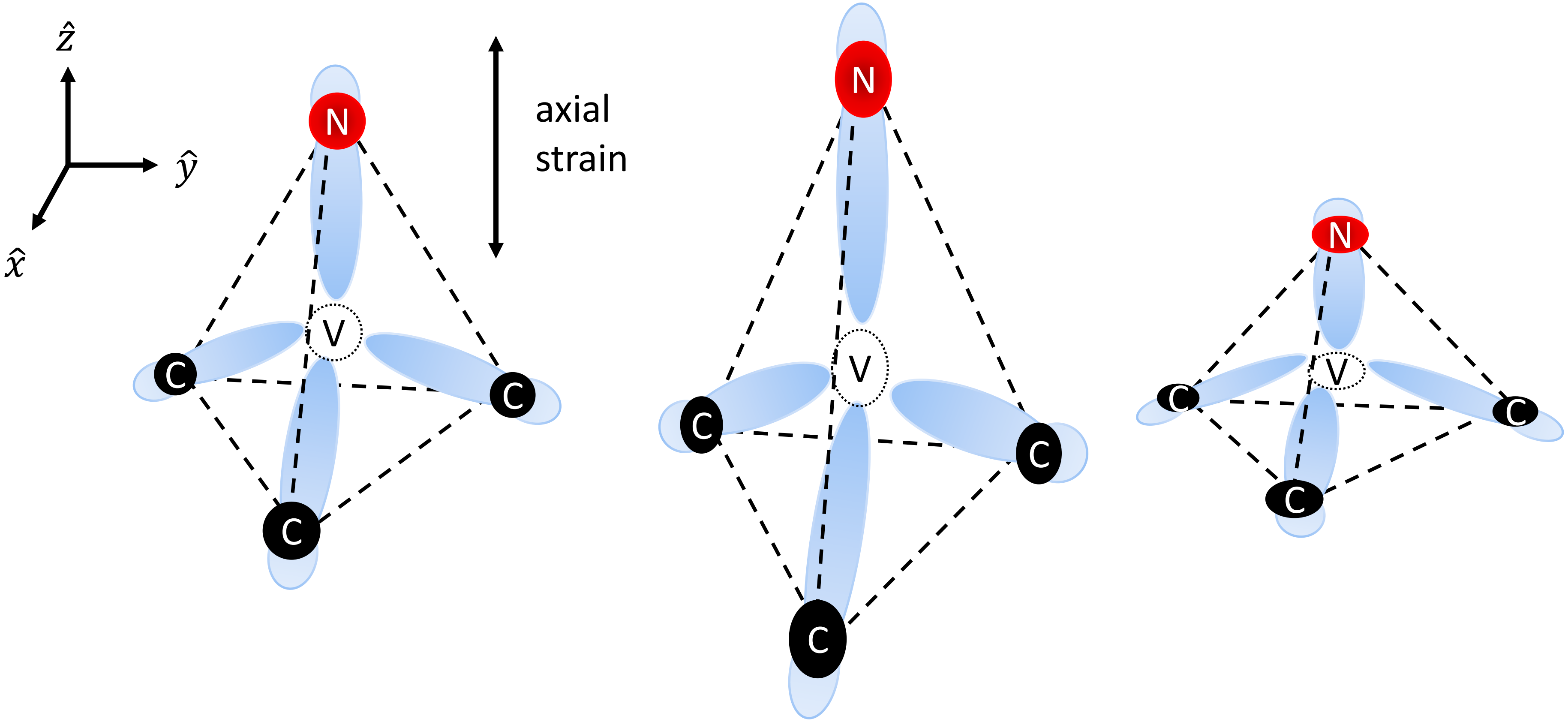

Energy levels change followed by C_{3v} symmetry group

- axial strain: uniform shift of all energy levels

Strain field sensing

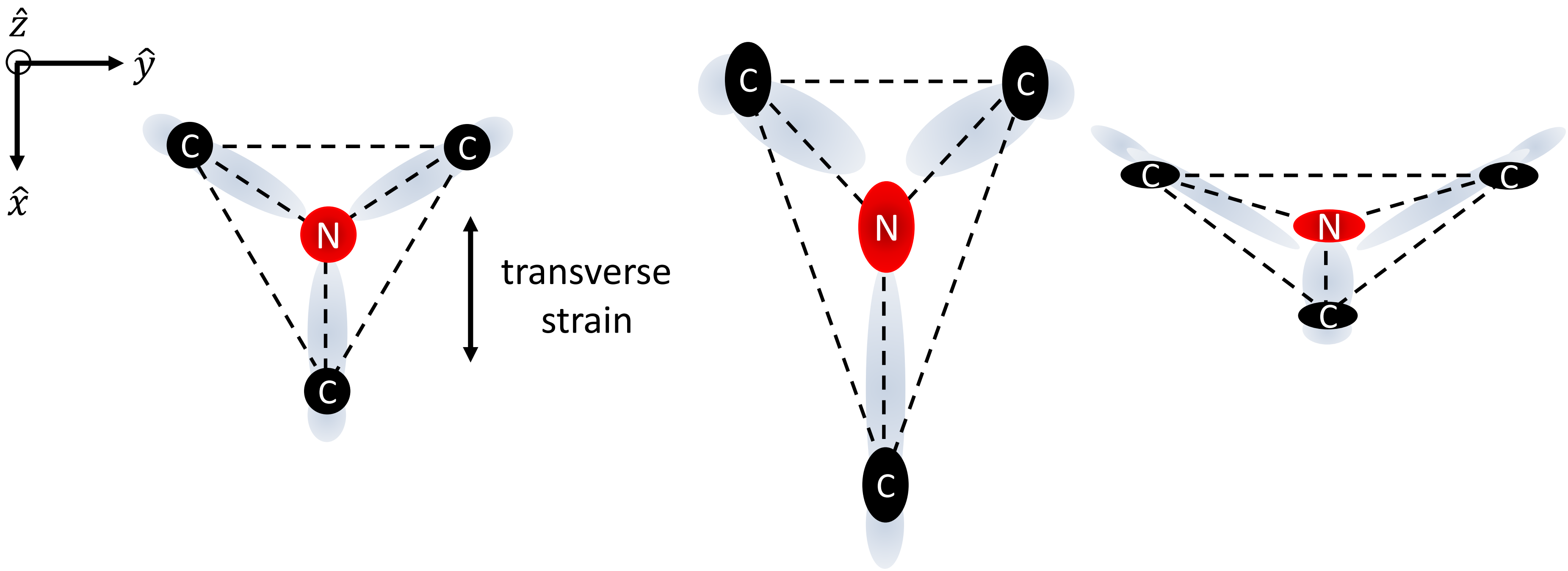

Energy levels change followed by C_{3v} symmetry group

- axial strain: uniform shift of all energy levels
- transverse strain: split and mix of energy levels (orbitals along $\hat{x}$ and $\hat{y}$)

Ground state Hamiltonian and energy level change

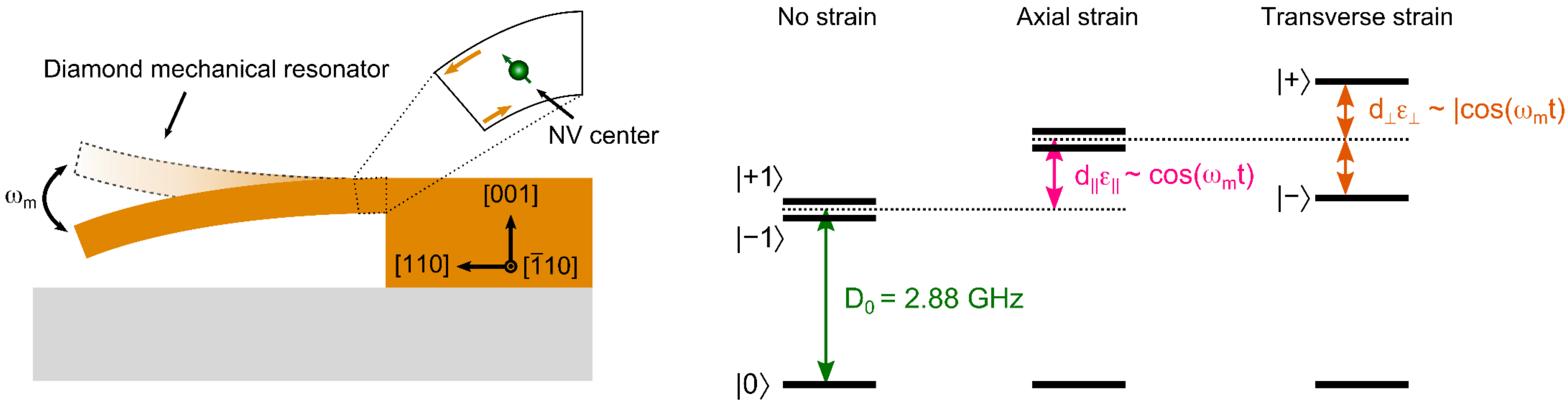

$$E_{\pm}(s) = D_0 + \boldsymbol{d_{\parallel}\varepsilon_{\parallel}} \pm \sqrt{(\boldsymbol{\gamma_{NV}B_z})^2 + (\boldsymbol{d_{\perp}\varepsilon_{\perp}})^2}$$

- AC parallel strain modulates at mechanical frequency
- AC perpendicular strain modulates at twice mechanical frequency

Axial strain detection with Hahn echo pulse sequence

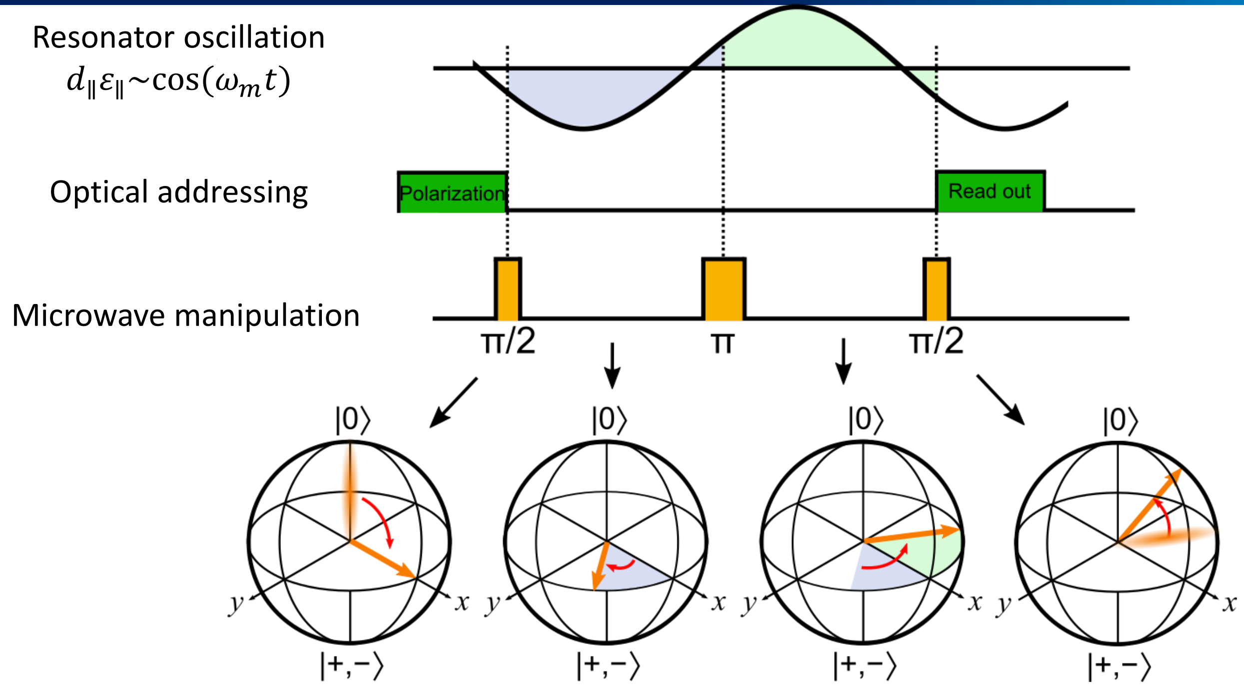

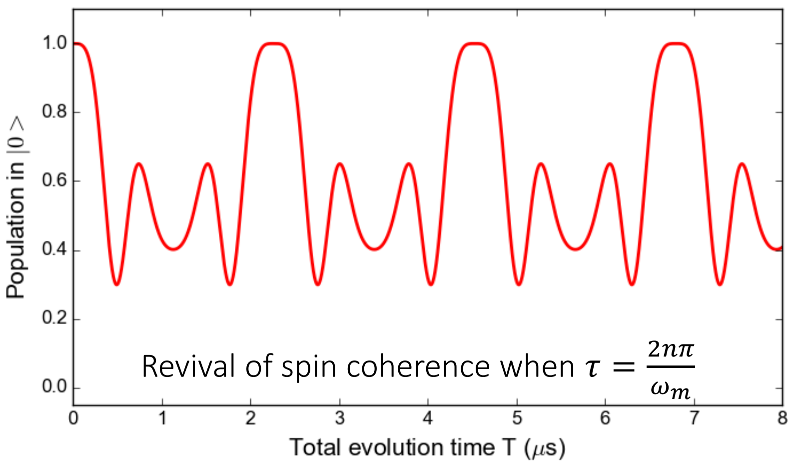

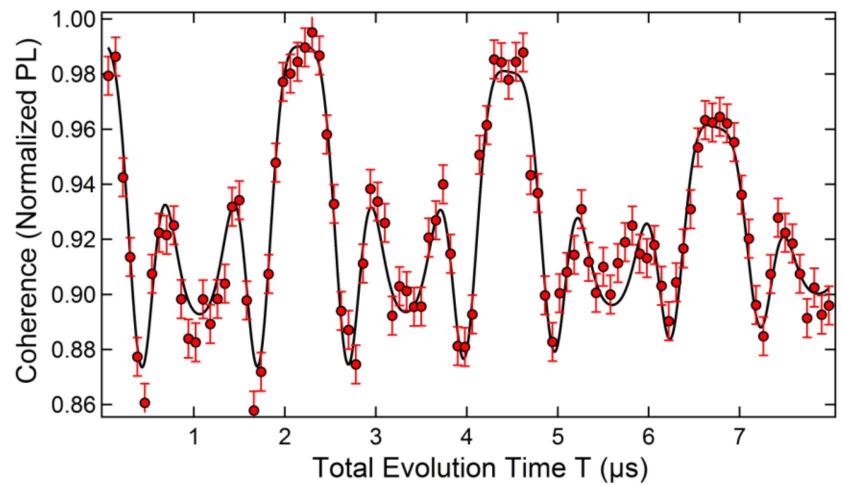

$d_{\parallel} = 13.4 \pm 0.8\ \mathrm{GHz/strain}$

P. Ovartchaiyapong *et al.*, Nat. Comm. (2014)

Transverse strain detection with XY-4 pulse sequence

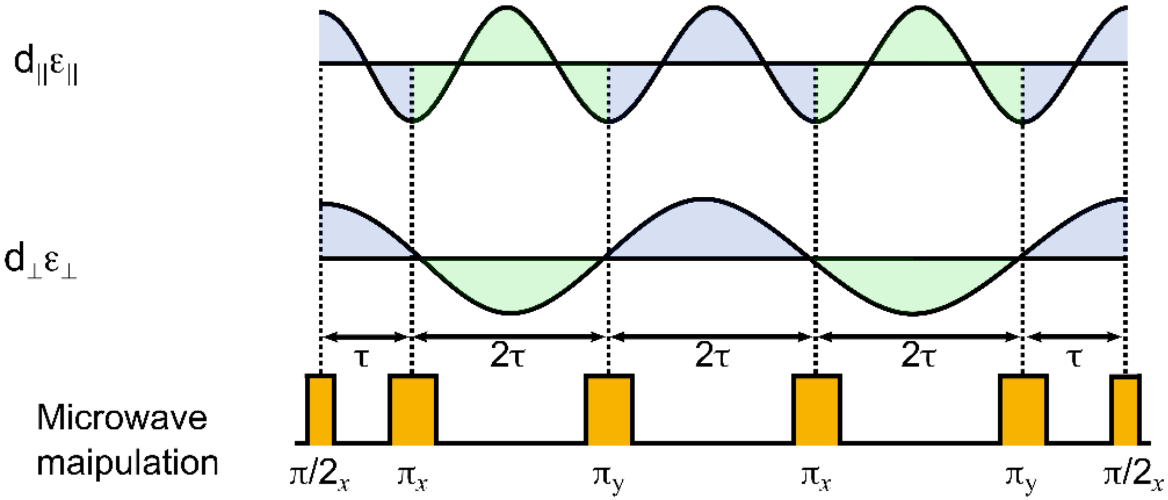

- XY-4 pulse sequence used
- Interference between axial strain ($\sim \omega_m$) and transverse strain ($\sim 2\omega_m$)

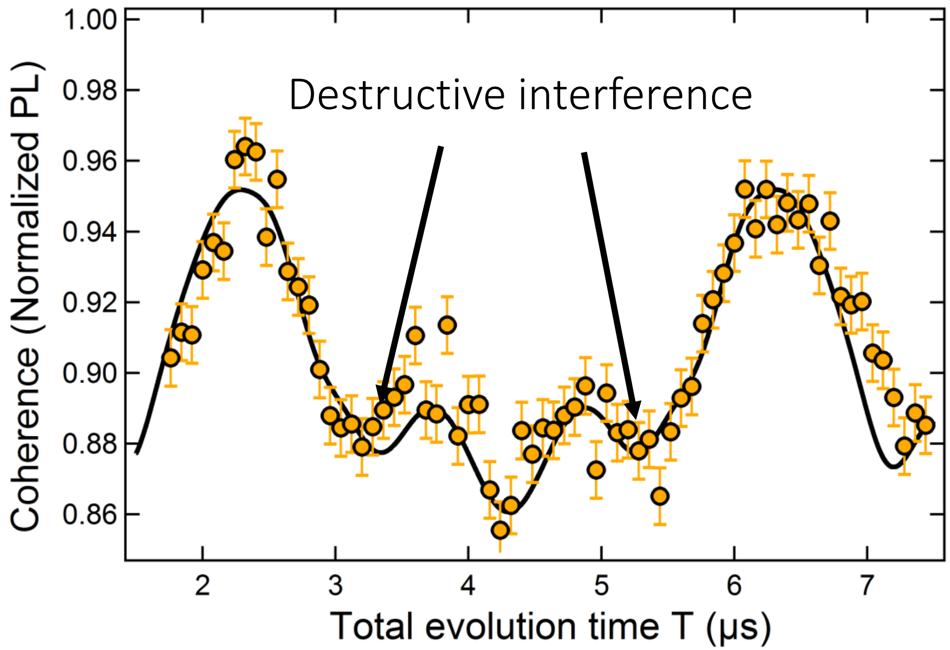

$d_{\perp} = 21.5 \pm 0.8\ \mathrm{GHz/strain}$

P. Ovartchaiyapong *et al.*, Nat. Comm. (2014)

Summary

- Basics of the NV center
  - Structure, electronic, optical properties
  - Spin physics, coherence properties
- Applications for quantum metrology
  - Magnetic field sensing
  - Strain field sensing
- Other applications (next time ?)